

1  
2  
3

4 **The transcription factor TRF2 has a unique function in regulating  
5 cell cycle and apoptosis**

6  
7  
8

9 Adi Kedmi\*, Anna Sloutskin\*, Natalie Epstein\*, Lital Gasri-Plotnitsky\*, Debby  
10 Ickowicz\*, Irit Shoval\*, Tirza Doniger\*, Eliezer Darmon\*, Diana Ideses\*, Ziv Porat†,  
11 Orly Yaron\*, and Tamar Juven-Gershon\*<sup>1</sup>

12  
13

14 \* The Mina and Everard Goodman Faculty of Life Sciences, Bar-Ilan University,  
15 Ramat Gan 5290002, Israel; and

16  
17 † The Flow Cytometry Unit, Life Sciences Core Facilities, Weizmann Institute of  
18 Science, Rehovot 7610001, Israel

19  
20 <sup>1</sup> Correspondence: The Mina and Everard Goodman Faculty of Life Sciences, Bar-  
21 Ilan University, Ramat Gan 5290002, Israel. E-mail: [tamar.gershon@biu.ac.il](mailto:tamar.gershon@biu.ac.il)

22  
23  
24  
25

26 **ABSTRACT**

27 **Background:** Diverse biological processes and transcriptional programs are  
28 regulated by RNA polymerase II (Pol II), which is recruited by the general transcription  
29 machinery to the core promoter to initiate transcription. TRF2 (TATA-box-binding  
30 protein-related factor 2) is an evolutionarily conserved general transcription factor that  
31 is essential for embryonic development of *Drosophila melanogaster*, *C. elegans*,  
32 zebrafish and *Xenopus*. Nevertheless, the cellular processes that are regulated by  
33 TRF2 are largely underexplored.

34 **Results:** Here, using *Drosophila* Schneider cells as a model, we discovered that TRF2  
35 regulates apoptosis and cell cycle progression. We show that TRF2 knockdown  
36 results in increased expression of distinct pro-apoptotic genes and induces apoptosis.  
37 Using flow cytometry, high-throughput microscopy and advanced imaging-flow  
38 cytometry, we demonstrate that TRF2 regulates cell cycle progression and exerts  
39 distinct effects on G1 and specific mitotic phases. RNA-seq analysis revealed that  
40 TRF2 controls the expression of *Cyclin E* and the mitotic cyclins, *Cyclin A*, *Cyclin B*  
41 and *Cyclin B3*, but not *Cyclin D* or *Cyclin C*. To identify proteins that could account for  
42 the observed regulation of these cyclin genes, we searched for TRF2-interacting  
43 proteins. Interestingly, mass spectrometry analysis of TRF2-containing complexes  
44 identified GFZF, a nuclear glutathione S-transferase implicated in cell cycle regulation,  
45 and Motif 1 binding protein (M1BP). TRF2 has previously been shown to interact with  
46 M1BP and M1BP has been shown to interact with GFZF. Furthermore, available ChIP-  
47 exo data revealed that TRF2, GFZF and M1BP co-occupy the promoters of TRF2-  
48 regulated genes. Using RNAi to knockdown the expression of either M1BP, GFZF,  
49 TRF2 or their combinations, we demonstrate that although GFZF and M1BP interact

50 with TRF2, it is TRF2, rather than GFZF or M1BP, that is the main factor regulating  
51 the expression of *Cyclin E* and the mitotic cyclins.

52 **Conclusions:** Our findings uncover a critical and unanticipated role of a general  
53 transcription factor as a key regulator of cell cycle and apoptosis.

54

55 **Keywords**

56 Basal transcription machinery, RNA polymerase II, gene expression, TATA box-  
57 binding protein (TBP), TBP-related factor 2 (TRF2), cyclin genes.

58

59 **BACKGROUND**

60 Multiple biological processes and transcriptional programs are regulated by RNA  
61 polymerase II (Pol II). The initiation of transcription of protein-coding genes and  
62 distinct non-coding RNAs occurs following the recruitment of Pol II to the core  
63 promoter region by the general/basal transcription machinery (1-4). The core  
64 promoter, which directs accurate initiation of transcription and encompasses the  
65 transcription start site (TSS), may contain short DNA sequence elements/motifs,  
66 which confer specific properties to the core promoter (1, 4-10). The first step in the  
67 recruitment of Pol II to initiate transcription is the binding of TFIID, which is  
68 composed of TATA-box-binding protein (TBP) and TBP-associated factors.

69 Remarkably, although TBP is considered a universal general transcription factor,  
70 robust Pol II transcription is observed in mouse TBP-/- blastocysts, indicating the  
71 existence of TBP-independent Pol II transcription *in vivo* (11). The complexity of  
72 transcription is also manifested by the existence of diverse transcriptional regulators,

73 among which are the TBP family members. There are three TBP family members in  
74 *Drosophila melanogaster*: TBP, TRF1 and TRF2 (reviewed in (12-16)). TRF1, the  
75 first *Drosophila* TBP family member identified, is insect specific (17). An evolutionary  
76 conservation analysis indicated that TRF2 (also known as TLP (TATA-like protein),  
77 TLF (TBP-like factor), TRP (TBP-related protein) and TBPL1 (TBP-like 1)), is highly  
78 conserved in evolution (12, 18-22) and is present in all bilaterian organisms, but not  
79 in any of the non-bilaterian genomes available (19). It was further discovered that  
80 TRF2, which is involved in Pol II transcription, evolved by duplication of the TBP  
81 gene (19). Yet, unlike TBP and TRF1, TRF2 does not bind TATA-box containing  
82 promoters (19, 20, 22). There are two *Drosophila* TRF2 protein isoforms that result  
83 from an internal translation initiation: the evolutionarily conserved short isoform (632  
84 aa; typically referred to as “TRF2”) and a long *Drosophila*-only isoform (1715 aa), in  
85 which the same short amino acid sequence is preceded by an N-terminal domain  
86 (23). TRF2 affects early embryonic development of *Drosophila*, *C. elegans*, zebrafish  
87 and *Xenopus*, differentiation and morphogenesis (23-32). Mouse TRF2 is essential  
88 for spermiogenesis (33-35).

89 One of the open questions in the transcriptional regulation field is what are the  
90 cellular functions of TRF2. Despite its importance in development, the cellular  
91 processes that are regulated by TRF2 remain largely underexplored. To identify and  
92 characterize the cellular processes that are regulated by TRF2, we used *Drosophila*  
93 S2R+ cells as a model and knocked-down the expression of TRF2. We discovered  
94 that reduced expression of TRF2 (but not TBP or TRF1) results in apoptosis and  
95 increased expression of key, yet not all, pro-apoptotic genes (including *rpr*, *hid*, *p53*),  
96 suggesting this is not a general stress response. Surprisingly, not only that TRF2  
97 regulates apoptotic cell death, reduced expression of TRF2 (but not its family

98 members, TBP or TRF1), exerts distinct effects on G1, G2/M and specific mitotic  
99 phases, as demonstrated by quantitative high-throughput imaging flow cytometry.  
100 We further discovered that TRF2 controls the expression of *Cyc E* and the mitotic  
101 *Cyc A*, *Cyc B* and *Cyc B3* genes. Using mass spectrometry analyses of TRF2-  
102 interacting proteins and available ChIP-exo data, we demonstrate the co-occupancy  
103 of TRF2, GFZF (GST-containing FLYWCH zinc-finger protein) and M1BP (motif 1  
104 binding protein) in the majority of promoters bound by each of the three factors.  
105 Remarkably, the promoters of the TRF2-regulated mitotic cyclins and *Cyclin E* are  
106 bound by the three factors, whereas the promoters of *Cyclin C* and *Cyclin D*, which  
107 are not regulated by TRF2, are not bound. Furthermore, the Motif 1 sequence  
108 element is enriched in the promoters of genes bound by all three proteins,  
109 suggesting the involvement of GFZF and M1BP as co-factors in TRF2-regulated cell  
110 cycle progression. Moreover, we demonstrate that TRF2, rather than M1BP or  
111 GFZF, is the main factor that regulates the expression of the mitotic cyclins and  
112 *Cyclin E*. Importantly, while general/basal transcription factors might be viewed as  
113 having a somewhat “generic” role, our findings emphasize the unique, unanticipated  
114 functions of *Drosophila* TRF2 as an essential factor for cell cycle progression and  
115 apoptotic cell death.

## 116 RESULTS

### 117 Knockdown of TRF2 expression results in apoptotic cell death and induced 118 expression of key pro-apoptotic genes

119 The TBP-related transcription factor TRF2 is a key general/basal transcription factor  
120 (reviewed in (12-16)), yet the cellular processes that are regulated by TRF2 remain  
121 largely underexplored. To investigate the cellular functions of TRF2, we used

122 *Drosophila* S2R+ cells as a model, and knocked down its expression by RNAi using  
123 non-overlapping dsRNA probes (Additional file 1: Figure S1a). TBP knockdown was  
124 used as a control throughout this study. The resulting reduction in protein expression  
125 was verified by western blot analysis (Additional file 1: Figure S1b, c). We  
126 consistently observed significant cell death following TRF2 knockdown, as evident by  
127 microscopic examination and by the reduced amounts of total RNA purified from  
128 TRF2-RNAi treated cells, as compared to mock-treated cells. To specifically  
129 investigate whether TRF2 plays an important role in apoptosis, we performed  
130 Annexin V/PI analysis to detect early and late apoptotic cell death by flow cytometry  
131 analysis. PI is excluded from cells with intact membranes, while dead and damaged  
132 cells have membranes that are permeable to PI. Annexin V binds phospholipids that  
133 are exposed in cells undergoing apoptosis. Hence, cells that are both Annexin V and  
134 PI negative are considered viable, while cells that are in early apoptosis are Annexin  
135 V positive and PI negative, and cells that are in late apoptosis or already dead are  
136 both Annexin V and PI positive. S2R+ cells were incubated for three days with either  
137 one of the four non-overlapping dsRNA probes directed against *Trf2*, a dsRNA probe  
138 against *Tbp*, a dsRNA probe against *Trf1* or a dsRNA probe against the  
139 homeodomain transcription factor *exd*, as a negative control. Cells were harvested  
140 and stained with Annexin-V FITC/PI. Approximately 30% of cells stain positive for  
141 Annexin V following TRF2 knockdown by the four different dsRNA probes, ~2 fold  
142 higher than the mock and the exd-RNAi treated cells (Fig. 1). Notably, cell death  
143 induced by TBP or TRF1 dsRNA probes (an average of 20%) was not as  
144 pronounced as the cell death induced by either of the four TRF2 dsRNA probes.  
145 These findings emphasize the unique effects of TRF2, as compared to TBP, on  
146 apoptosis.

147 To identify the targets that are unique to TRF2, we used RNAi to knockdown  
148 either TRF2 or TBP in *Drosophila* S2R+ cells and performed RNA-seq analysis at  
149 two time points, 48h and 72h. In order to further understand how TRF2 knockdown  
150 results in cell death, we searched our RNA-seq data for pro-apoptotic genes that are  
151 regulated by TRF2. The inhibitor of apoptosis protein (IAP) family has already been  
152 shown to play an important role in cell survival (reviewed in (36-38)). *Drosophila*  
153 Death-associated IAP-1 (DIAP1), a key member of the IAP family, inhibits apoptosis  
154 by binding to the active Caspase 9-like Dronc, and functioning as an E3-ubiquitin  
155 ligase to promote its degradation. The *reaper* (*rpr*), *head involution defective* (*hid*),  
156 and *grim* genes encode IAP antagonists that bind DIAP1, disrupt its interactions with  
157 caspases and target it for degradation, resulting in caspase activation and cell death.  
158 Scylla (*scyl*) has been implicated in developmental cell death (39). Indeed, the RNA-  
159 seq analysis revealed a significant upregulation of *rpr* and *scyl* (Additional file 2:  
160 Table S1). We thus decided to knockdown either TRF2 (probes #1 and #2), exd,  
161 TBP or TRF1 and examine by reverse transcription-qPCR the expression of multiple  
162 genes implicated in the apoptotic machinery: the IAP antagonists *rpr*, *hid* and *grim*  
163 (reviewed in (37)), *scyl* (39), the BCL-2 family members *buffy* (40) and *Death*  
164 *executioner Bcl-2 (Debcl)* (41-44), and the Caspase 9-like *Dronc* (reviewed in (37)).  
165 Remarkably, reducing the expression levels of TRF2 (but not exd, TBP or TRF1)  
166 resulted in increased expression levels of *rpr*, *hid* and *scyl* (Fig. 2a). The detected  
167 increase in *Buffy* expression levels was not statistically significant. The expression of  
168 *grim*, *Debcl* and *Dronc* was not significantly altered by TRF2 knockdown (Fig. 2a),  
169 suggesting that this is not a general stress response, and that TRF2 specifically  
170 regulates the expression of distinct, but not all, pro-apoptotic genes.

171           The p53 tumor suppressor gene is a key regulator of both cell cycle  
172           progression and programmed cell death (reviewed, for example, in (45, 46)). p53 is  
173           expressed at low levels in S2R+ cells ([www.flybase.org](http://www.flybase.org)). Surprisingly, the RNA-seq  
174           analysis revealed its upregulation upon TRF2 knockdown (Additional file 2: Table  
175           S1). Examination of p53 expression by reverse transcription-qPCR following  
176           knockdown of either TRF2 (probes #1 and #2) or TBP reproduced the upregulation  
177           trend of p53 expression by TRF2. Notably, TBP knockdown did not alter the  
178           expression of p53, manifesting the unique characteristics of gene regulation via  
179           TRF2. Interestingly, it was previously demonstrated that p53 regulates the  
180           expression of *rpr* and *hid*, which in turn, induce apoptosis (47, 48). Hence, it is  
181           possible that the observed upregulation of *rpr* and *hid* following the knockdown of  
182           TRF2 (Fig. 2a, b) is mediated via p53. Unfortunately, multiple attempts to reduce the  
183           levels of endogenous p53 by two different dsRNA probes, were unsuccessful. Thus,  
184           one cannot exclude the possibility that the increased expression of p53 following  
185           TRF2 knockdown, may partially contribute to the upregulation of *rpr* and *hid*  
186           expression.

187

188           **TRF2 exerts distinct effects that are independent of TBP**

189           TRF2 may repress transcription involving TBP or TFIID, probably by recruiting TFIIA  
190           (20, 49). One can suggest that TRF2 is, in some respects, antagonistic to TBP, and  
191           the observed upregulation of pro-apoptotic genes following TRF2 knockdown (Fig. 2)  
192           results from TBP activity, which is no longer obstructed by TRF2. To examine  
193           whether the observed upregulation of *rpr* and *hid* results from TBP activity, we  
194           overexpressed TBP in S2R+ cells that were either incubated with TRF2 dsRNA  
195           probes or mock treated. Although overexpression of TBP was clearly evident (>100

196 fold; Additional file 3: Figure S2), no differences in the levels of *rpr* and *hid* were  
197 observed upon its overexpression (Additional file 3: Figure S2). Furthermore,  
198 overexpression of TBP following TRF2 knockdown did not alter *rpr* or *hid* expression.  
199 Thus, we conclude that the observed upregulation of *rpr* and *hid* following TRF2  
200 knockdown results from the activity of TRF2 as a unique transcription factor, rather  
201 than a TBP antagonist.

202

203 **Knockdown of endogenous TRF2 expression results in altered cell cycle  
204 distribution and G1 arrest**

205 To identify specific cellular processes that are regulated by TRF2, we performed  
206 Gene Ontology (GO) terms analysis of genes that were either downregulated or  
207 upregulated following TRF2 knockdown (using string.db.org). Surprisingly, we  
208 discovered that genes that were downregulated following TRF2 knockdown are  
209 enriched for cell cycle and mitotic cell cycle processes, while genes that were  
210 upregulated following TRF2 knockdown are enriched for response to stimulus and  
211 stress (Additional file 2: Table S1). Interestingly, while the number of genes that were  
212 downregulated was only half of the number of the upregulated genes following TRF2  
213 knockdown (337 vs. 684 genes, respectively), the enrichment scores (-log<sub>10</sub>(P  
214 values)) of the downregulated genes were 5-fold higher. We thus decided to  
215 examine the effects of TRF2 knockdown on cell cycle distribution. To knockdown the  
216 expression of the endogenous genes, S2R+ cells were incubated for three days with  
217 dsRNA probes against *Trf2*, *Tbp*, *Trf1* or *exd*, as a negative control. Cells were  
218 harvested, fixed and analyzed by flow cytometry. Control S2R+ cells display a  
219 normal profile with an average of ~31% of cells in G1 phase and with an average of  
220 ~34% of cells in G2/M phase, similarly to mock treated cells (which were processed

221 similarly, but were not incubated with any dsRNA; Fig. 3). Following TRF2  
222 knockdown by either one of the four dsRNA probes, we observed a distinct decrease  
223 in the fraction of cells in G2/M phase (an average of ~20%), as well as the fraction of  
224 cells in S phase (an average of ~20%) with a concomitant increase in the fraction of  
225 cells in G1 phase (an average of ~55%). Remarkably, these effects are unique to  
226 TRF2 knockdown, as the knockdown of its family members TBP or TRF1 resembles  
227 the cell cycle distribution of control and mock treated cells (Fig. 3).

228 Our RNA-seq analysis reveals subsets of genes that are involved in S and  
229 G2/M phases. In addition, the cell cycle analysis indicates that TRF2 plays a role in  
230 S and/or G2/M phases. To determine if TRF2 affects cell cycle progression to S  
231 phase, S2R+ cells were arrested in G1 with 1mM hydroxyurea (HU) for 18h following  
232 knockdown of either TRF2 (dsRNA probes #1 and #2) or TBP, and then released to  
233 cycle by replacing the medium with fresh medium. As can be seen in Figure 4, HU  
234 treatment (0h) resulted in accumulation of cells in G1 (~55%). Two hours following  
235 the release, mock treated cells returned to cycle (indicated by the decrease in the  
236 number of cells in G1), and the fraction of cells in S and G2/M increased. Similarly,  
237 cells in which TBP was depleted by RNAi, returned to cycle. Surprisingly, unlike  
238 mock or TBP RNAi-treated cells, cells in which TRF2 was depleted by either one of  
239 the two probes, remained in G1 (~55%) and did not return to cycle (Fig. 4, Additional  
240 file 4: Figure S3). Moreover, even 8h following the removal of HU, cells in which  
241 TRF2 was knocked-down remained G1-arrested. Our findings imply that  
242 endogenous TRF2 is involved in progression into S phase.

243  
244  
245

246 **TRF2 regulates the expression of specific cyclin genes**

247 To further explore the connection between TRF2 and cell cycle progression, we  
248 turned to our RNA-seq data for cell cycle-related genes that may be influenced by  
249 knockdown of TRF2. We discovered that following TRF2 knockdown, the expression  
250 of the *Cyc A*, *Cyc B*, *Cyc B3* and *Cyc E* cell cycle regulators was significantly  
251 reduced (over 2.3-fold). Notably, the expression levels of *Cyc C* and *Cyc D* were  
252 unchanged (Additional file 2: Table S1). In order to verify the effect of TRF2  
253 knockdown on the expression of these genes, reverse transcription-qPCR analysis  
254 of endogenous cyclin genes was performed on mock, TRF2 (probes #1 and #2), exd,  
255 TBP or TRF1 RNAi-treated cells. Knockdown of TRF2 by either probe #1 or #2  
256 significantly reduces the expression of *Cyc A*, *Cyc B* and *Cyc B3*, as compared to  
257 mock treated cells, much more than knockdown of TBP or TRF1 (Fig. 5a). As there  
258 was a difference between the effects of probe #1 and #2 on *Cyc E* expression, 4  
259 non-overlapping TRF2 dsRNA probes were used to assess the effect of TRF2  
260 knockdown on *Cyc E* expression (Fig. 5b). Notably, each of the 4 non-overlapping  
261 TRF2 dsRNA probes reduces *Cyc E* expression. Unlike *Cyc D* (which is required for  
262 G1 progression (50, 51)), the expression of *Cyc E* (which promotes G1-S transition  
263 (52, 53)) was reduced following TRF2 knockdown (Fig. 5a, b). We next tested  
264 whether TRF2 knockdown affects the protein levels of *Cyc A*, *Cyc B* and *Cyc E*.  
265 Unfortunately, we were unable to detect endogenous *Cyc A* and *Cyc B* protein  
266 expression using publicly available anti-*Drosophila* *Cyc A* and *Cyc B* antibodies  
267 (data not shown). Remarkably, using anti-*Drosophila* *Cyc E* antibodies, we observed  
268 a distinct reduction in *Cyc E* protein levels following knockdown of TRF2 (but not  
269 TBP), using both TRF2 probes (Fig. 5c), further suggesting that TRF2 regulates G1-  
270 S transition by modulating the expression of *Cyc E*.

271 **TRF2 regulates distinct mitotic phases**

272 We were intrigued by the downregulation of the mitotic cyclin gene expression (*Cyc*  
273 *A*, *Cyc B* and *Cyc B3*) following TRF2 knockdown (Fig. 5a) and decided to explore  
274 the effect of TRF2 downregulation on mitotic phases. To this end, we knocked-down  
275 the expression of TRF2 or TBP and stained cells for mitotic chromatin (anti-phospho-  
276 Histone H3 (Ser10)), DNA (Hoechst) and filamentous Actin (Phalloidin). These  
277 allowed us to analyze the fraction of cells in mitosis following TRF2 knockdown (Fig.  
278 6a). To determine the number of mitotic cells, we developed a pipeline to  
279 automatically detect the Hoechst and phospho-Histone H3 signals. Notably, there  
280 was a reduction in the number of cells undergoing mitosis following TRF2  
281 knockdown, as compared to mock or TBP RNAi treated cells (Fig. 6b).

282 To explore the effect of TRF2 on G2/M, we sought to synchronize cells in  
283 G2/M. Unfortunately, we were unable to synchronize cells in G2/M in a reversible  
284 manner (see methods), and thus we could not perform G2/M block-release  
285 experiments. Nevertheless, we succeeded in discerning the effects of TRF2 on  
286 specific mitotic phases by employing advanced imaging-flow cytometry analysis  
287 (ImageStreamX mark II imaging flow-cytometer, Amnis Corp, Seattle, WA, Part of  
288 EMD Millipore). Imaging-flow cytometry analysis combines the high-quality imaging  
289 and functional insights of microscopy with the speed, sensitivity, and phenotyping  
290 abilities of flow cytometry. We knocked down the expression of TRF2 or TBP and  
291 stained cells with anti-phospho-Histone H3 (Ser10) antibodies and Hoechst. A total  
292 of 40,000 cells of each treatment were analyzed by an ImageStream flow cytometer  
293 to determine the number of cells in each mitotic phase, according to their nuclear  
294 morphology (Fig. 6c-f, Additional file 5: Figure S4, Additional file 6: Table S2).  
295 Remarkably, although 40,000 cells were analyzed in each experiment, only a few

296 hundred cells were mitotic, and following TRF2 knockdown there was an even bigger  
297 reduction in the total number of mitotic cells (Fig. 6b, d). Notably, despite the overall  
298 reduction in the mitotic cell population, knockdown of TRF2 (but not TBP) resulted in  
299 a significant accumulation of cells in anaphase and telophase (Fig. 6e, f).

300 To validate the accurate identification of mitotic cells, we used Colchicine as a  
301 control. Colchicine treatment resulted in accumulation of cells in mitosis, specifically  
302 in anaphase (Fig. 6e). Multiple studies have shown that Colchicine disrupts the  
303 metaphase to anaphase transition (see for example, (54)), yet, the increase in  
304 anaphase has also been documented (55). Furthermore, it is established that  
305 different cell types behave differently during mitosis in the presence of drugs that  
306 disrupt microtubules function (56). Interestingly, morphological examination of the  
307 Colchicine-treated S2R+ cells indicated aberrant DNA staining patterns and mal-  
308 oriented clumped chromosomes in prophase, metaphase and anaphase cells  
309 (Additional file 7: Figure S5), in line with the absence of a spindle. Notably, mal-  
310 oriented un-centered chromosomes, such as those observed in Colchicine-treated  
311 cells, were not observed in TRF2-RNAi treated cells.

312

313 **The effects of TRF2 knockdown on cyclin gene expression correlates with the  
314 promoter occupancies of TRF2 and its co-factors GFZF and M1BP**

315 To better understand how TRF2 regulates the expression of the cyclin genes, we  
316 turned our attention to TRF2-interacting proteins. TRF2 was recently shown to  
317 interact with M1BP (motif 1 binding protein) (57). Interestingly, M1BP was recently  
318 demonstrated to interact with GFZF, a nuclear glutathione S-transferase protein that  
319 has been implicated in cell cycle regulation (58). We suspected that GFZF may  
320 interact with TRF2. Indeed, using FLAG immuno-affinity purification from FLAG-HA

321 TRF2-inducible S2R+ cells followed by mass spectrometry analysis, we discovered  
322 that both M1BP and GFZF are in complex with the evolutionarily conserved TRF2  
323 (also known as short TRF2), but not with the long *Drosophila*-only TRF2 isoform or  
324 with TBP (Table 3 and Additional file 8: Table S3). This prompted us to examine the  
325 occupancy of TRF2, M1BP and GFZF in the vicinity of the TSSs (-100 to +100  
326 relative to the TSS) of TRF2-regulated cyclin genes, using publicly available TRF2,  
327 M1BP and GFZF ChIP-exo analyses in *Drosophila* S2R+ cells (GSE97841,  
328 GSE105009) (57, 58). We examined the number of bound sites, the average peak  
329 scores and the maximum peak scores of cyclin genes and several ribosomal protein  
330 genes for comparison (Table 4). As expected, M1BP, TRF2 and GFZF co-occupy  
331 the promoters of the ribosomal protein genes. Interestingly, while M1BP occupies the  
332 -100 to +100 regions of all the examined cyclin genes, both TRF2 and GFZF occupy  
333 the -100 to +100 regions of Cyc A, Cyc B, Cyc B3 and Cyc E, and to a lesser extent  
334 the promoters of Cyc C and Cyc D, which are not regulated by TRF2. The  
335 occupancies of the three proteins is especially striking in the vicinities of the Cyc B  
336 and Cyc B3 TSSs. Thus, the effects of TRF2 knockdown on cyclin gene expression  
337 generally correlate with the occupancies of both TRF2 and GFZF in the -100 to +100  
338 regions of Cyc A, Cyc B, Cyc B3 and Cyc E.

339

340 To characterize the co-occupancies of TRF2, GFZF and M1BP in a genome-  
341 wide manner, we examined the binding of each factor to *Drosophila* promoter  
342 regions ( $\pm$  50 bp relative to FlyBase annotated TSSs). Remarkably, a major fraction  
343 of promoters is bound by all three transcription factors (Fig. 7a). Reassuringly, the  
344 co-bound promoters include the TRF2-regulated Cyc A, Cyc B, Cyc B3 and Cyc E,  
345 but not Cyc C and Cyc D promoters, which are not regulated by TRF2.

346 To better decipher the characteristics of the co-bound promoters, we used MEME  
347 (59) to detect enriched sequence motifs. Interestingly, the top enriched motif in  
348 promoters that are bound by all three proteins (Fig. 7b) closely resembles Ohler  
349 Motif 1 (60), also detected in M1BP ChIP-exo analysis (57). We next analyzed the  
350 core promoter composition of the co-bound promoters, using the ElemeNT algorithm  
351 (61). Strikingly, the co-bound promoters are depleted for the TATA-box motif and  
352 enriched for the TCT and Motif 1 core promoter elements, as compared to the  
353 genomic distribution of core promoter elements (Fig. 7c).

354 To examine the contribution of M1BP and GFZF to the effect of TRF2  
355 knockdown on cyclin gene expression, we used RNAi to knockdown the expression  
356 of either M1BP, GFZF, TRF2 or their combinations. The use of each of the dsRNA  
357 probes resulted in a significantly reduced expression of the targeted gene (Fig. 7d).  
358 Surprisingly, M1BP knockdown resulted in increased expression of *Trf2*, *gfzf* and  
359 *Cyc E*. Since both TRF2 and M1BP were previously shown to affect the expression  
360 of ribosomal protein genes (32, 62), we tested whether their knockdown affects the  
361 expression of several ribosomal target genes, namely, *RpL30*, *RpLP1* and *RpLP2*.  
362 While TRF2 and GFZF knockdown did not affect their expression, M1BP knockdown  
363 resulted in significantly increased expression of *RpLP2* (Additional file 9: Figure  
364 S6a). Notably, this effect was not general, but rather specific to distinct cyclin and  
365 ribosomal protein genes (Fig. 7d, e and Additional file 9: Figure S6), as the  
366 expression of *CG12493* and *SgII*, two previously identified M1BP targets (62), was  
367 reduced following M1BP knockdown (Additional file 9: Figure S6b).  
368 The expression levels of *Cyc A* and *Cyc B* were specifically reduced following TRF2  
369 knockdown, but not following GFZF or M1BP knockdown (Fig. 5a and Fig. 7d, e).  
370 *Cyc D* expression was not affected by either of these single factor knockdowns (Fig.

371 7d), as in Figure 5. As can be observed by TRF2 knockdown, as well as the  
372 combined knockdown of TRF2, GFZF and M1BP, the expression pattern of *Cyc A*  
373 and *Cyc B* are mostly influenced by TRF2 knockdown. *Cyc E* exhibits a composite  
374 pattern: it is reduced following TRF2 knockdown, but the combined knockdowns of  
375 TRF2 and M1BP or GFZF seem to restore its expression as compared to mock  
376 treatment. Notably, *Cyc D* expression pattern is the least affected by the different  
377 knockdown combinations.

378        Taken together, these data suggest that the observed effects of TRF2  
379 knockdown on cell cycle progression (Figs. 3, 4 and 6) are, at least partially,  
380 mediated by the reduced expression of *Cyc E*, *Cyc A* and *Cyc B* following TRF2  
381 knockdown (Figs. 5 and 7d, e). Importantly, the co-occupancy of TRF2, GFZF and  
382 M1BP in the promoters of these cyclin genes, the enrichment of Motif 1 in their  
383 promoters and the expression patterns of the cyclin genes following the knockdown  
384 of either TRF2 alone, or in combination with GFZF and/or M1BP, imply that GFZF  
385 and M1BP may serve as co-factors in TRF2-regulated cell cycle progression. Yet, it  
386 is TRF2 that is the major transcription factor regulating the expression pattern of the  
387 abovementioned cyclin genes.

388

## 389 **DISCUSSION**

390 In this study, we discovered that knockdown of the general/basal transcription factor  
391 TRF2 results in increased expression of the *rpr*, *hid* and *p53* pro-apoptotic genes,  
392 which is in line with the observed increased apoptotic cell death following TRF2  
393 knockdown and with the extensively characterized involvement of p53 in apoptosis,

394 G1 arrest and G2 arrest (reviewed, for example, in (45)). A recent study has  
395 demonstrated that human TRF2 interferes with MDM2 binding and ubiquitination of  
396 p53, leading to p53 protein stabilization (63). Our results provide evidence for  
397 another level of p53 regulation, *i.e.*, transcriptional regulation. Furthermore, in a  
398 similar manner to the p53-MDM2 negative feedback loop in vertebrates (reviewed in  
399 (45)), activation of *Drosophila* p53 transcriptionally activates the *companion of reaper*  
400 (*corp*) gene (64-66), which in turn, negatively regulates its activity (67). The fact that  
401 *corp* expression in *Drosophila* S2R+ is rather low and not altered by TRF2  
402 knockdown (Additional file 2: Table S1), may provide support for p53-independent  
403 regulation of *rpr* and *hid* by TRF2.

404 Furthermore, we examined the expression of multiple additional genes  
405 implicated in apoptosis following TRF2 knockdown. *Scylla* is pro-apoptotic (39) and  
406 its upregulation is in line with the observed cell death following TRF2 knockdown.  
407 *Buffy*, a *Drosophila* Bcl2 family member, however, has been shown to act in an anti-  
408 apoptotic manner, but has also been shown to cause a G1-S arrest (40). Thus, its  
409 upregulation following TRF2 knockdown may contribute to the observed G1-S  
410 accumulation of cells. These effects are in line with studies suggesting the existence  
411 of TRF2-regulated transcriptional systems (10, 16, 32, 68, 69) and are unlikely to  
412 represent a general stress response, as the expression of *Debcl* and *Dronc* is not  
413 affected by TRF2 knockdown.

414 Interestingly, we discovered that TRF2 knockdown results in accumulation of  
415 cells in G1 and in reduction in the number of cells in S and G2/M phases. G1/S  
416 transition is regulated by Cyclin E activity, while S phase and G2/M transition are  
417 regulated by Cyclin A activity, and transition into and within mitosis is regulated by

418 the activities of Cyclin B and Cyclin B3. Remarkably, TRF2 knockdown in S2R+ cells  
419 resulted in reduced expression of Cyc E, Cyc A, Cyc B and Cyc B3 (but not Cyc D),  
420 suggesting that TRF2 regulates cell cycle progression by modifying the expression of  
421 specific cyclins. The reduced expression of Cyc A, Cyc B and Cyc B3 and the  
422 reduction of the number of cells undergoing mitosis following TRF2 knockdown, are  
423 in line with previous studies, which demonstrated inhibition of nuclear mitotic entry in  
424 *Drosophila* embryos following simultaneous knockdown of Cyc A, Cyc B and Cyc B3  
425 (70). Interestingly, Cyclin A and Cyclin B have previously been shown to inhibit  
426 metaphase-anaphase transition, whereas Cyclin B3 promotes it (71). Thus, the  
427 specific accumulation of cells in anaphase and telophase observed by imaging flow  
428 cytometry (Fig. 6e, f), could result from the reduced expression of Cyc A and Cyc B  
429 following TRF2 knockdown (Fig. 5). Notably, to the best of our knowledge, this study  
430 is the first to employ imaging-flow cytometry in the analysis of *Drosophila* cells.

431 To examine whether TRF2-interacting proteins could account for the observed  
432 regulation of Cyc E, Cyc A, Cyc B and Cyc B3 (but not Cyc D or Cyc C), we  
433 searched for TRF2-interacting proteins. TRF2 has been shown to interact with M1BP  
434 (57) and M1BP has been shown to interact with GFZF, a nuclear glutathione S-  
435 transferase implicated in cell cycle regulation (57). Our proteomic analyses revealed  
436 that both M1BP and GFZF preferentially interact with TRF2, but not with TBP (Table  
437 3 and Additional file 8: Table S3). Remarkably, examination of publicly available  
438 TRF2, M1BP and GFZF ChIP-exo data from *Drosophila* S2R+ cells (57, 58),  
439 indicated that the effects of TRF2 knockdown on the expression of cyclin genes  
440 correlate with TRF2, GFZF and M1BP co-occupancies of the promoters of the TRF2-  
441 regulated cyclin genes (Table 4), in line with the reported regulatory effects of  
442 GFZF. Genome-wide examination of promoters bound by all three transcription

443 factors revealed the enrichment of the TCT and Motif 1 core promoter elements.  
444 Whereas one would expect the TCT to be enriched as TRF2 and M1BP have  
445 previously been implicated in the regulation of ribosomal protein genes (32), the  
446 enrichment of Motif 1 within promoters bound by all three factors indicates a shared  
447 function for TRF2, GFZF and M1BP. Notably, in our experimental system, TRF2  
448 knockdown by RNAi resulted in a two-fold reduction in *Trf2* levels (Fig. 2a, Additional  
449 file 2: Table S1). Under these conditions, we did not detect any change in ribosomal  
450 protein gene expression (Additional file 2: Table S1). Hence, the reduced expression  
451 of *Cyc A*, *Cyc B* and *Cyc E* following a two-fold reduction in TRF2 expression, does  
452 not result from a general inhibition of protein synthesis. As direct binding of TRF2 to  
453 DNA could not be demonstrated (32), it is likely that TRF2 indirectly regulates the  
454 expression of these cyclin genes and that there are TRF2-associated factors that  
455 enable DNA binding. Our analysis suggested that GFZF and M1BP could serve as  
456 such factors for specific TRF2-regulated processes. Interestingly, the expression  
457 patterns of the cyclin genes following the knockdown of either TRF2 alone, or in  
458 combination with GFZF and/or M1BP, indicated that among these three factors,  
459 TRF2 is the major contributor to the expression pattern of *Cyc A*, *Cyc B* and *Cyc E*.  
460 Moreover, while *Cyclin A*, *Cyclin B* and *Cyclin E* expression levels are reduced  
461 following TRF2 (but not GFZF) knockdown, the expression levels of both *Cyclin A*  
462 and *Cyclin B*, but not *Cyclin E*, are reduced following the combined knockdown of  
463 TRF2 and GFZF (Fig. 7d, e), suggesting that the reduced expression levels of *Cyclin*  
464 *A* and *Cyclin B* are not mediated via *Cyclin E*.

465 Notably, mouse TBP was recently shown to remain bound to mitotic  
466 chromosomes during mitosis of mouse embryonic stem cells (mESCs), and to recruit  
467 a small population of Pol II molecules to mitotic chromosomes (72). Nevertheless,

468 active Pol II transcription occurs in the absence of mouse TBP, whereas Pol I and  
469 Pol III, are significantly reduced (11, 72). It remains to be determined whether  
470 *Drosophila* TBP is bound to mitotic chromosomes during mitosis. As we did not  
471 observe significant effects on cell cycle progression or mitosis following *Drosophila*  
472 TBP knockdown (Figs. 3, 4 and 6), it is likely that *mouse* TBP may exert different  
473 functions as compared to *Drosophila* TBP, perhaps via its associated proteins.

474 The effects of TRF2 knockdown on cell cycle progression and apoptosis of  
475 *Drosophila* cultured S2R+ cells are in line with the early embryonic lethality of TRF2  
476 knockout flies. TRF2 has also been shown to be essential for embryonic  
477 development of *C. elegans*, zebrafish and *Xenopus*. It remains to be determined  
478 whether knockdown of TRF2 in cellular systems from these species results in similar  
479 effects.

## 480 CONCLUSIONS

481 Taken together, using *Drosophila* cells as a model system, we discovered that the  
482 knockdown of TRF2, rather than TBP or TRF1, regulates apoptosis and cell cycle  
483 progression via distinct target genes. Importantly, we discovered that TRF2 is  
484 associated with the GFZF and M1BP proteins, and that TRF2, GFZF and M1BP co-  
485 occupy the promoters of the TRF2-regulated cyclins. Furthermore, we show that  
486 TRF2, rather than GFZF or M1BP, is the major contributor to the expression pattern  
487 of Cyc E, Cyc A and Cyc B. Importantly, while a general transcription factor may be  
488 regarded as having a “generic function”, our findings emphasize the unique,  
489 unanticipated functions of *Drosophila* TRF2 as an essential factor for specific major  
490 cellular processes.

491 **MATERIALS AND METHODS**

492

493 ***Drosophila melanogaster* Schneider S2R+ Cells**

494 *Drosophila melanogaster* Schneider S2R+ adherent cells were cultured in

495 Schneider's *Drosophila* Media (Biological Industries) that was supplemented with

496 10% heat-inactivated FBS and Penicillin 100 units/ml Streptomycin 0.1mg/ml

497 (Biological Industries).

498

499 **Generation of dsRNA probes**

500 All dsRNA probes were chosen based on <http://www.dkfz.de/signaling/e-rnai3/> and

501 <http://www.flyrnai.org/snapdragon> as described in (69). Primer sequences used for

502 the generation of dsRNA probes are provided in Table 1. DNA fragments

503 corresponding to each dsRNA were subcloned into both pBlueScript SK+ and KS+.

504 The dsRNA probes were generated by PCR amplification of the DNA using T7 and

505 T3 primers, followed by *in vitro* transcription of templates in both pBlueScript

506 orientations using T7 RNA polymerase. Resulting RNA products were annealed to

507 generate the dsRNA probes.

508

509 **RNA interference (RNAi)**

510 For 6 well plate,  $1.25 \times 10^6$  cells/well were resuspended and seeded in empty

511 Schneider's *Drosophila* Media (Biological Industries) with 30 $\mu$ g/ml dsRNA directed

512 against different genes for 1 hour. Next, two volumes of complete medium were

513 added to the wells and cells were incubated for 3 additional days.

514

515

516

517 **Western blot analysis**

518 Knockdown of TRF2 and TBP was verified by western blot analysis using anti-TRF2  
519 and anti-TBP polyclonal antibodies (generous gift from Jim Kadonaga). Cyclin E  
520 levels were analyzed by the 8B10 antibodies (generous gift from Helena Richardson)  
521 (73). The levels of Actin or  $\gamma$ -Tubulin, as a loading control, were detected using either  
522 mouse monoclonal anti-Actin (Abcam, 8224) or anti-  $\gamma$ -Tubulin (Sigma, GTU-88)  
523 antibodies. Anti-Cyclin A and -Cyclin B concentrated monoclonal antibodies  
524 (Developmental Studies Hybridoma Bank, A12 and F2F4, respectively) were tested  
525 as well, however no endogenous proteins were detected, possibly due to technical  
526 limitations.

527

528 **TBP expression vector**

529 The coding sequence of *Drosophila* TBP was amplified by PCR and cloned with an  
530 N-terminal Flag-HA tag into the pAc5.1 vector (Life Technologies) using cDNA from  
531 S2R+ cells as template and the following primers: Forward (containing an Xhol site,  
532 underlined)  
533 5' CCGCTCGAGGACCAAATGCTAAGCCCCA 3' and reverse (containing an AgeI  
534 site, underlined) 5' AGCACCGGTTTATGACTGCTTCTTGAACCTCTTTAA 3'  
535 Plasmid sequence was verified by sequencing.

536 **RNAi-coupled overexpression**

537 For 6 well plate,  $1.25 \times 10^6$  *Drosophila* S2R+ cells/well were resuspended and seeded  
538 in empty medium with 30 $\mu$ g/ml dsRNA directed against TRF2 for 1 hour. Next, two  
539 volumes of complete medium were added to the wells and cells were incubated for 3  
540 days. Three days post dsRNA treatment, cells were transfected with the TBP-pAc  
541 expression vector (930 ng) or an empty vector control using the Escort IV reagent

542 (Sigma). Media was replaced 18-24 hrs post transfection. Cells were harvested 36-  
543 48 hrs post transfection and RNA was purified and analyzed by RT-qPCR. Each  
544 qPCR experiment was performed in triplicates. The graphs represent an average of  
545 3 independent experiments. Error bars represent SEM.

546

#### 547 **RNA-seq analysis**

548 S2R+ cells were treated with dsRNA probes against *Trf2* (probe #1) and *Tbp*, and  
549 harvested at two time points - 48h and 72h post RNAi treatment. For each time point,  
550 a matched mock control was collected separately.

551 RNA was extracted using Quick-RNA™ MiniPrep (Zymo Research), and 800ng of  
552 each sample was purified using NEBNext Poly(A) mRNA Magnetic Isolation Module  
553 (NEB #E7490). Libraries were prepared using NEBNext Ultra II RNA Library Prep Kit  
554 for Illumina (NEB #E7770), following the manufacturer's instructions. NEBNext  
555 Multiplex Oligos for Illumina (NEB #E7335, NEB #E7500, NEB #E7710, NEB  
556 #E7730) were used. Libraries were pooled and a 1% PhiX library control was added.  
557 Single-end sequencing was performed on an Illumina NextSeq 500 machine.

558 Reads were aligned to dm6 genome build using STAR (version 2.6.0a), and htseq-  
559 count (version 0.5.1p3, (74)) was used to count the reads mapped to each gene.

560 Differential expression analysis of conditions was performed using the DESeq2 R  
561 package (75). Only genes with adjusted p-value < 0.1 were considered for  
562 subsequent analysis. GO terms analysis was carried out using STRING v11 (76).  
563 For all experiments, three independent biological replicates were compared and  
564 merged for subsequent analysis. RNA-seq Data is available at GSE133685.

565

566

567 **RT-PCR**

568 Total RNA was isolated using the PerfectPure RNA Cultured Cell kit (5 PRIME) or  
569 Quick-RNA™ MiniPrep (Zymo Research). One microgram of the total RNA was  
570 reverse-transcribed into cDNA with M-MLV (Promega) or qScript Flex cDNA Kit  
571 (Quanta). Control reactions lacking reverse transcriptase were also performed to  
572 ensure that the levels of contaminating genomic DNA were negligible. Quantitation  
573 was performed by real-time PCR to determine the transcription levels of the  
574 endogenous genes. The expression levels were compared to *Gapdh2*. Primer  
575 sequences for real-time PCR are provided in Table 2. For all quantifications, the  
576 error bars represent  $\pm$ S.E.M of at least 3 independent experiments; NS, not  
577 significant; \*\* $P < 0.01$ ; \*\*\* $P < 0.001$ . Statistical analyses were performed on log-  
578 transformed relative quantification (RQ) values using one-way ANOVA followed by  
579 Tukey's post hoc test, unless otherwise stated in the figure legend.

580

581 **Flow cytometry analysis**

582 For cell cycle distribution by Propidium Iodide (PI) staining, cells were harvested  
583 following 72h incubation with dsRNA, centrifuged for 5 min at 300g and fixed with  
584 80% ethanol at 4°C overnight. Before subjecting the cells to flow cytometry, the cells  
585 were centrifuged for 5 min at 300g, washed in 1 ml of Phosphate-buffered saline  
586 (PBS) and incubated for 40 min at 4°C. The cells were then stained in PBS  
587 containing 50 µg/ml PI (Sigma) and 50 µg/ml RNase A (Roche). After incubation for  
588 15 min at room temperature, fluorescence was measured using a FACSCalibur  
589 Becton Dickinson flow cytometer.

590 For analyzing apoptosis by Annexin V and PI staining, cells were harvested 72h  
591 following incubation with dsRNA probes and stained with Annexin V and PI

592 (MEBCYTO Apoptosis Kit; MBL). Fluorescence was measured using a FACSCalibur  
593 Becton Dickinson flow cytometer.  
594 For G1 phase cell arrest by hydroxyurea (HU) and BrdU (5-Bromo-2'-Deoxyuridine)-  
595 PI staining, 72h following incubation with dsRNA, the medium was replaced with  
596 medium containing a final concentration of 1mM HU for 18h (77) (for control cells,  
597 the medium was replaced with a fresh medium). BrdU (40µM final concentration)  
598 was added to the medium for 2h. Cells were released from HU by medium  
599 replacement and, at 0, 2, 4, 6 or 8 hours following the release, cells were harvested,  
600 centrifuged and fixed with 80% ethanol at 4°C overnight. Following fixation, cells  
601 were stained with FITC (*Fluorescein isothiocyanate*)-conjugated anti-BrdU antibodies  
602 (BD) and PI according to the provided protocol, and fluorescence was measured  
603 using BD FACSARIA III. All flow cytometry data was analyzed using the FlowJo  
604 software. Statistical analyses of flow cytometry and imaging flow cytometry data  
605 were performed in SPSS using two-tailed Students t-test. The number of times each  
606 experiment was repeated, is detailed in the figure legends.

607 It is of note that unfortunately, we were unable to synchronize cells in G2/M in  
608 a reversible manner using either Nocodazole or Colchicine, which cause  
609 microtubules depolymerization. Specifically, Nocadazole did not arrest the S2R+  
610 cells in G2/M, while Colchicine, which has been used since the 1950s to inhibit  
611 mitotic progression, did cause enrichment of mitotic cells (Fig. 6b, d). However, this  
612 effect was irreversible (data not shown). Thus, Colchicine could not be used for  
613 G2/M block-release synchronization experiments.

614  
615

616 **Immunostaining for fluorescence microscopy and Imaging flow cytometry  
617 analysis**

618 Cells were RNAi-treated as described above. On day 4, 2ml of fresh medium was  
619 added to the wells. To enrich for G2/M, as a control, Colchicine (Sigma) was added  
620 to a final concentration of 350ng/ml. On the following day, the cells were harvested  
621 and fixed with 4% Paraformaldehyde (PFA)/PBS (30 min), washed in PBST (PBS  
622 containing 0.5% Triton x), blocked with PBS containing 1% BSA and 1% serum (1h),  
623 and incubated with phospho-Histone H3 (Ser10) antibody (1:200, Cell Signaling  
624 Technology #9701) for 1h at RT, followed by overnight at 4°C. Cells were washed,  
625 stained with the secondary antibody (1:500, DyLight 488, ab96883), and then  
626 counter-stained with 10µg/ml Hoechst 33342 (Sigma). For microscopy analysis,  
627 samples were also stained for filamentous Actin with 3.5µM Acti-stain 670 Phalloidin  
628 (Cytoskeleton, Inc. Cat. # PHDN1). Following staining, samples were subjected to  
629 imaging flow cytometry, confocal microscopy or wide-field fluorescence microscopy  
630 analysis.

631

632 **Microscope image analyses**

633 High resolution images were acquired using a Leica SP8 confocal microscope, and  
634 high-throughput images for quantitative analysis were acquired using a Leica DMi8  
635 microscope. Three separate experiments were performed and captured at 20x  
636 magnification. For each treatment, approximately 275 frames were acquired and  
637 analysed. The total number of Alexa 488 anti-phosphor-Histone H3 (Ser10) (PH3)  
638 labeled cells, and the total number of Hoechst stained cells, were calculated using  
639 the Fiji distribution of ImageJ.

640 Analysis workflow:

641 1. The raw PH3 channel images were enhanced using brightness and contrast, and  
642 then the background was subtracted by reducing the Gaussian blurred filtered  
643 image of the enhanced image. Next, a median filter was applied to smoothen the  
644 image and an Otsu threshold was applied to get the binary image of all mitotic  
645 nuclei. Finally, watershed was implemented to separate touching nuclei. Mitotic  
646 cells were counted, eliminating small debris and noise.

647 2. To analyze the Hoechst channel, the background was subtracted by reducing the  
648 Gaussian blurred filtered image of the original image. Next, a Moments threshold  
649 was applied to get the binary image of total nuclei. Finally, watershed was  
650 implemented to separate touching nuclei. Nuclei were counted while eliminating  
651 small debris and noise.

652 The ratio between the number of mitotic cells and the total number of cells yields the  
653 mitotic index for each treatment.

654 All manipulations in the images were made evenly across the entire field.

655 The Fiji macros will be shared upon request.

656

### 657 **Multispectral imaging flow-cytometry (IFC) analysis**

658 Cells were imaged using multispectral imaging flow cytometry (ImageStreamX mark  
659 II imaging flow-cytometer; Amnis Corp, Seattle, WA, Part of EMD Millipore). Each  
660 experiment was performed 3 times. In each experiment, at least 40,000 cells were  
661 collected from each sample, and data were analyzed using the image analysis  
662 software (IDEAS 6.2; Amnis Corp). Images were compensated for fluorescent dye  
663 overlap by using single-stain controls. Imaging flow cytometry results were analyzed  
664 by calculation of a set of parameters, termed “features”, performed on a defined area  
665 of interest, termed “mask”. The serial gating strategy to identify the mitotic cell

666 population was as follows: Single cells were first gated using the area and aspect  
667 ratio features on the bright-field (BF) image (the aspect ratio, which indicates how  
668 round or oblong an object is, is calculated by division of the minor axis by the major  
669 axis). Uncropped cells were gated using the centroid X (the number of pixels in the  
670 horizontal axis from the upper left corner of the image to the center of the mask) and  
671 area features. Focused cells were gated using the Gradient RMS feature, as  
672 previously described (78) (Additional file 5: Figure S4a-c). Following this standard  
673 gating series, the mitotic cell fraction of the entire cell population was identified using  
674 the staining intensity for PH3 AF488 (channel 2), and mitotic cells were gated as the  
675 high intensity population of PH3 staining within all focused cells (Additional file 5:  
676 Figure S4d,e).

677 For a more complex analysis, we performed a second gating series. Focused cells  
678 were first gated for G2/M based on DNA (Hoechst) intensity (Additional file 5: Figure  
679 S4) and then gated for mitotic cells, as previously, by high PH3 intensity. To further  
680 subdivide into the specific cell division phases, we gated according to nuclear  
681 morphology based on the spot count and aspect ratio intensity features (see  
682 Additional file 5: Figure S4f, g for detailed masking and gating). As it was previously  
683 shown that serine 10 of histone H3 becomes dephosphorylated during telophase  
684 (79), the telophase population was derived from the negative PH3-stained cells,  
685 based on the BF circularity feature and DNA aspect ratio intensity (see Additional file  
686 5: Figure S4h for detailed masking and gating). Full details of all masking, features  
687 and analysis strategies are included in the legend of Additional file 5: Figure S4.

688 **Identification of unique TRF2-interacting proteins**

689 To identify the proteins that are in complex with TRF2 (the evolutionarily conserved  
690 short TRF2), we used inducible FLAG-HA-tagged TRF2 S2R+ cells (69). As

691 controls, we used inducible S2R+ for FLAG-HA-long TRF2 (69) or FLAG-HA-TBP  
692 (generated as in (69)). Cells were either induced by copper sulfate or left untreated.  
693 Protein extracts were prepared and TRF2-containing complexes were immuno-  
694 precipitated using anti-FLAG M2 affinity gel (Sigma). Following the IP, TRF2-  
695 containing complexes were released with a FLAG peptide (Sigma). Samples were  
696 resolved by SDS-PAGE. Proteins that were purified from TRF2-induced cells were  
697 separated to two samples: proteins larger or smaller than 40 kDa. Samples were  
698 subjected to Mass spectrometry analyses (The Smoler Protein Research Center,  
699 Technion). Briefly, samples were digested by trypsin, analyzed by LC-MS/MS on Q-  
700 Exactive Plus (ThermoFisher) and identified by the Discoverer software (with two  
701 search algorithms: Sequest (ThermoFisher) and Mascot (Matrix science) against the  
702 *Drosophila melanogaster* section of the NCBI non-redundant and Uniprot databases,  
703 and a decoy database (in order to determine the false discovery rate). All the  
704 identified peptides were filtered with high confidence, top rank, mass accuracy, and a  
705 minimum of 2 peptides. High confidence peptides have passed the 1% FDR  
706 threshold. Semi-quantitation was done by calculating the peak area of each peptide.  
707 The area of the protein is the average of the three most intense peptides from each  
708 protein. The results are provided in Additional file 8: Table S3.

709

## 710 **Visualization of publicly available ChIP-exo data**

711 A genome browser session  
712 ([https://genome.ucsc.edu/s/Anna%20Sloutskin/dm3\\_ChIP\\_Exo](https://genome.ucsc.edu/s/Anna%20Sloutskin/dm3_ChIP_Exo)) based on available  
713 TRF2, GFZF and M1BP ChIP-exo bedgraph files (GSE97841, GSE105009) (57, 58)  
714 was created. The session contains an “Overlap” track (the ChIP-exo peaks that were  
715 identified as overlapping in the ±50bp window relative to FlyBase TSS) and the

716 “trustedTSS” track that is based on 5' GRO-seq (GSE68677) and PRO-Cap  
717 (GSM1032759) data. The relevant interval ( $\pm 50\text{bp}$  or  $100\text{bp}$ ) is indicated.

718

719 **List of abbreviations**

720 ChIP-exo - chromatin immunoprecipitation combined with exonuclease digestion  
721 followed by high-throughput sequencing

722 DPE - downstream core promoter element

723 GFZF - GST-containing FLYWCH zinc-finger protein

724 M1BP - Motif 1 binding protein

725 Pol II - RNA polymerase II

726 TBP - TATA-box-binding protein

727 TRF2 - TBP-related factor 2

728 TSS - Transcription start site

729

730

731 **Declarations**

732 **Ethics approval and consent to participate**

733 Not applicable

734

735 **Consent for publication**

736 Not applicable

737

738 **Availability of data and materials**

739 RNAseq data generated during the current study is available in the GEO repository  
740 (GSE133685).

741 ChIP-exo data analyzed during the current study was downloaded from the GEO  
742 (GSE97841, GSE105009).

743

744 **Competing interests**

745 The authors declare that they have no competing interests

746

747 **Funding**

748 This work was supported by grants from the Israel Science Foundation to T.J.-G.  
749 (no. 798/10 and no. 1234/17).

750

751 **Authors' contributions**

752 A. Kedmi prepared RNA samples and O. Yaron and A. Sloutskin performed RNA-  
753 seq experiments. T. Doniger and A. Sloutskin analyzed the RNA-seq experiments  
754 and performed bioinformatics analysis. A. Kedmi, N. Epstein, L. Gasri-Plotnitsky and  
755 D. Ickowicz performed and/or analyzed flow cytometry experiments. A. Kedmi, A.  
756 Sloutskin and D. Ideses performed reverse transcription-qPCR analysis. I. Shoval  
757 and Z. Porat advised and performed the analysis of ImageStream® experiments, A.  
758 Kedmi and I. Shoval performed and analyzed fluorescence microscopy experiments.  
759 E. Darmon and D. Ideses performed western blot analyses. A. Sloutskin performed  
760 the statistical analysis. A. Kedmi, A. Sloutskin and T. Juven-Gershon designed the  
761 study, planned experiments, analyzed results, and wrote the manuscript with input  
762 from all authors.

763

764

765

766 **Acknowledgements**

767 We thank Jim Kadonaga for the generous gift of anti-TRF2 and anti-TBP antibodies,  
768 for invaluable advice and assistance and for critical reading of the manuscript. We  
769 thank Helena Richardson for the generous gift of anti-Cyclin E antibodies. We thank  
770 Moshe Oren, Doron Ginsberg, Ze'ev Paroush, Sivan Henis-Korenblit, Shaked Cohen  
771 and Itay Lazar for invaluable advice and assistance. We thank Dr. Jennifer Israel-  
772 Cohen for assistance with statistical analysis. We thank Doron Ginsberg, Yaron  
773 Shav-Tal, Galit Shohat-Ophir and Orit Adato for critical reading of the manuscript.  
774 We thank Orit Adato and Sarit Lampert for technical assistance.

775

## 776 REFERENCES

- 777 1. Danino YM, Even D, Ideses D, Juven-Gershon T. The core promoter: At the  
778 heart of gene expression. *Biochimica et biophysica acta*. 2015;1849(8):1116-31.
- 779 2. Goodrich JA, Tjian R. Unexpected roles for core promoter recognition factors in  
780 cell-type-specific transcription and gene regulation. *Nature reviews Genetics*.  
781 2010;11(8):549-58.
- 782 3. Muller F, Tora L. Chromatin and DNA sequences in defining promoters for  
783 transcription initiation. *Biochimica et biophysica acta*. 2014;1839(3):118-28.
- 784 4. Thomas MC, Chiang CM. The general transcription machinery and general  
785 cofactors. *Crit Rev Biochem Mol Biol*. 2006;41(3):105-78.
- 786 5. Dikstein R. The unexpected traits associated with core promoter elements.  
787 *Transcription*. 2011;2(5):201-6.
- 788 6. Haberle V, Stark A. Eukaryotic core promoters and the functional basis of  
789 transcription initiation. *Nature reviews Molecular cell biology*. 2018;19(10):621-  
790 37.
- 791 7. Kadonaga JT. Perspectives on the RNA polymerase II core promoter. *Wiley  
792 Interdiscip Rev Dev Biol*. 2012;1(1):40-51.
- 793 8. Lenhard B, Sandelin A, Carninci P. Metazoan promoters: emerging  
794 characteristics and insights into transcriptional regulation. *Nature reviews  
795 Genetics*. 2012;13(4):233-45.
- 796 9. Ohler U, Wasserman DA. Promoting developmental transcription. *Development*.  
797 2010;137(1):15-26.
- 798 10. Vo Ngoc L, Wang YL, Kassavetis GA, Kadonaga JT. The punctilious RNA  
799 polymerase II core promoter. *Genes & development*. 2017;31(13):1289-301.
- 800 11. Martjanov I, Viville S, Davidson I. RNA polymerase II transcription in murine cells  
801 lacking the TATA binding protein. *Science*. 2002;298(5595):1036-9.
- 802 12. Akhtar W, Veenstra GJ. TBP-related factors: a paradigm of diversity in  
803 transcription initiation. *Cell & bioscience*. 2011;1(1):23.
- 804 13. Muller F, Zaucker A, Tora L. Developmental regulation of transcription initiation:  
805 more than just changing the actors. *Current opinion in genetics & development*.  
806 2010;20(5):533-40.
- 807 14. Reina JH, Hernandez N. On a roll for new TRF targets. *Genes & development*.  
808 2007;21(22):2855-60.
- 809 15. Torres-Padilla ME, Tora L. TBP homologues in embryo transcription: who does  
810 what? *EMBO reports*. 2007;8(11):1016-8.
- 811 16. Zehavi Y, Kedmi A, Ideses D, Juven-Gershon T. TRF2: TRansForming the view  
812 of general transcription factors. *Transcription*. 2015;0.
- 813 17. Hansen SK, Takada S, Jacobson RH, Lis JT, Tjian R. Transcription properties of  
814 a cell type-specific TATA-binding protein, TRF. *Cell*. 1997;91(1):71-83.
- 815 18. Dantone JC, Wurtz JM, Poch O, Moras D, Tora L. The TBP-like factor: an  
816 alternative transcription factor in metazoa? *Trends in biochemical sciences*.  
817 1999;24(9):335-9.
- 818 19. Duttke SH, Doolittle RF, Wang YL, Kadonaga JT. TRF2 and the evolution of the  
819 bilateria. *Genes & development*. 2014;28(19):2071-6.
- 820 20. Moore PA, Ozer J, Salunek M, Jan G, Zerby D, Campbell S, et al. A human  
821 TATA binding protein-related protein with altered DNA binding specificity inhibits  
822 transcription from multiple promoters and activators. *Molecular and cellular  
823 biology*. 1999;19(11):7610-20.

- 824 21. Persengiev SP, Zhu X, Dixit BL, Maston GA, Kittler EL, Green MR. TRF3, a  
825 TATA-box-binding protein-related factor, is vertebrate-specific and widely  
826 expressed. *Proceedings of the National Academy of Sciences of the United*  
827 *States of America*. 2003;100(25):14887-91.
- 828 22. Rabenstein MD, Zhou S, Lis JT, Tjian R. TATA box-binding protein (TBP)-related  
829 factor 2 (TRF2), a third member of the TBP family. *Proceedings of the National*  
830 *Academy of Sciences of the United States of America*. 1999;96(9):4791-6.
- 831 23. Kopytova DV, Krasnov AN, Kopantceva MR, Nabirochkina EN, Nikolenko JV,  
832 Maksimenko O, et al. Two isoforms of *Drosophila* TRF2 are involved in  
833 embryonic development, premeiotic chromatin condensation, and proper  
834 differentiation of germ cells of both sexes. *Molecular and cellular biology*.  
835 2006;26(20):7492-505.
- 836 24. Bashirullah A, Lam G, Yin VP, Thummel CS. dTrf2 is required for transcriptional  
837 and developmental responses to ecdysone during *Drosophila* metamorphosis.  
838 *Developmental dynamics : an official publication of the American Association of*  
839 *Anatomists*. 2007;236(11):3173-9.
- 840 25. Dantonel JC, Quintin S, Lakatos L, Labouesse M, Tora L. TBP-like factor is  
841 required for embryonic RNA polymerase II transcription in *C. elegans*. *Molecular*  
842 *cell*. 2000;6(3):715-22.
- 843 26. Jacobi UG, Akkers RC, Pierson ES, Weeks DL, Dagle JM, Veenstra GJ. TBP  
844 paralogs accommodate metazoan- and vertebrate-specific developmental gene  
845 regulation. *The EMBO journal*. 2007;26(17):3900-9.
- 846 27. Kaltenbach L, Horner MA, Rothman JH, Mango SE. The TBP-like factor CeTLF  
847 is required to activate RNA polymerase II transcription during *C. elegans*  
848 embryogenesis. *Molecular cell*. 2000;6(3):705-13.
- 849 28. Levine M, Cattoglio C, Tjian R. Looping back to leap forward: transcription enters  
850 a new era. *Cell*. 2014;157(1):13-25.
- 851 29. Muller F, Lakatos L, Dantonel J, Strahle U, Tora L. TBP is not universally  
852 required for zygotic RNA polymerase II transcription in zebrafish. *Current biology*  
853 : CB. 2001;11(4):282-7.
- 854 30. Neves A, Eisenman RN. Distinct gene-selective roles for a network of core  
855 promoter factors in *Drosophila* neural stem cell identity. *Biology open*. 2019;8(4).
- 856 31. Veenstra GJ, Weeks DL, Wolffe AP. Distinct roles for TBP and TBP-like factor in  
857 early embryonic gene transcription in *Xenopus*. *Science*. 2000;290(5500):2312-  
858 5.
- 859 32. Wang YL, Duttke SH, Chen K, Johnston J, Kassavetis GA, Zeitlinger J, et al.  
860 TRF2, but not TBP, mediates the transcription of ribosomal protein genes.  
861 *Genes & development*. 2014;28(14):1550-5.
- 862 33. Martjanov I, Fimia GM, Dierich A, Parvinen M, Sassone-Corsi P, Davidson I.  
863 Late arrest of spermiogenesis and germ cell apoptosis in mice lacking the TBP-  
864 like TLF/TRF2 gene. *Molecular cell*. 2001;7(3):509-15.
- 865 34. Zhang D, Penttila TL, Morris PL, Roeder RG. Cell- and stage-specific high-level  
866 expression of TBP-related factor 2 (TRF2) during mouse spermatogenesis.  
867 *Mechanisms of development*. 2001;106(1-2):203-5.
- 868 35. Zhang D, Penttila TL, Morris PL, Teichmann M, Roeder RG. Spermiogenesis  
869 deficiency in mice lacking the Trf2 gene. *Science*. 2001;292(5519):1153-5.
- 870 36. Deveraux QL, Reed JC. IAP family proteins--suppressors of apoptosis. *Genes &*  
871 *development*. 1999;13(3):239-52.

- 872 37. Fuchs Y, Steller H. Live to die another way: modes of programmed cell death  
873 and the signals emanating from dying cells. *Nature reviews Molecular cell*  
874 *biology*. 2015;16(6):329-44.
- 875 38. Martin SJ. Destabilizing influences in apoptosis: sowing the seeds of IAP  
876 destruction. *Cell*. 2002;109(7):793-6.
- 877 39. Scuderi A, Simin K, Kazuko SG, Metherall JE, Letsou A. scylla and charybde,  
878 homologues of the human apoptotic gene RTP801, are required for head  
879 involution in *Drosophila*. *Dev Biol*. 2006;291(1):110-22.
- 880 40. Quinn L, Coombe M, Mills K, Daish T, Colussi P, Kumar S, et al. Buffy, a  
881 *Drosophila* Bcl-2 protein, has anti-apoptotic and cell cycle inhibitory functions.  
882 *The EMBO journal*. 2003;22(14):3568-79.
- 883 41. Brachmann CB, Jassim OW, Wachsmuth BD, Cagan RL. The *Drosophila* bcl-2  
884 family member dBorg-1 functions in the apoptotic response to UV-irradiation.  
885 *Current biology : CB*. 2000;10(9):547-50.
- 886 42. Colussi PA, Quinn LM, Huang DC, Coombe M, Read SH, Richardson H, et al.  
887 Debcl, a proapoptotic Bcl-2 homologue, is a component of the *Drosophila*  
888 melanogaster cell death machinery. *The Journal of cell biology*.  
889 2000;148(4):703-14.
- 890 43. Igaki T, Kanuka H, Inohara N, Sawamoto K, Nunez G, Okano H, et al. Drob-1, a  
891 *Drosophila* member of the Bcl-2/CED-9 family that promotes cell death.  
892 *Proceedings of the National Academy of Sciences of the United States of  
893 America*. 2000;97(2):662-7.
- 894 44. Zhang H, Huang Q, Ke N, Matsuyama S, Hammock B, Godzik A, et al.  
895 *Drosophila* pro-apoptotic Bcl-2/Bax homologue reveals evolutionary conservation  
896 of cell death mechanisms. *The Journal of biological chemistry*.  
897 2000;275(35):27303-6.
- 898 45. Levine AJ, Oren M. The first 30 years of p53: growing ever more complex. *Nat  
899 Rev Cancer*. 2009;9(10):749-58.
- 900 46. Vousden KH, Lane DP. p53 in health and disease. *Nature reviews Molecular cell*  
901 *biology*. 2007;8(4):275-83.
- 902 47. Brodsky MH, Nordstrom W, Tsang G, Kwan E, Rubin GM, Abrams JM.  
903 *Drosophila* p53 binds a damage response element at the reaper locus. *Cell*.  
904 2000;101(1):103-13.
- 905 48. Fan Y, Lee TV, Xu D, Chen Z, Lamblin AF, Steller H, et al. Dual roles of  
906 *Drosophila* p53 in cell death and cell differentiation. *Cell Death Differ*.  
907 2010;17(6):912-21.
- 908 49. Teichmann M, Wang Z, Martinez E, Tjernberg A, Zhang D, Vollmer F, et al.  
909 Human TATA-binding protein-related factor-2 (hTRF2) stably associates with  
910 hTFIIA in HeLa cells. *Proceedings of the National Academy of Sciences of the  
911 United States of America*. 1999;96(24):13720-5.
- 912 50. Baldin V, Lukas J, Marcote MJ, Pagano M, Draetta G. Cyclin D1 is a nuclear  
913 protein required for cell cycle progression in G1. *Genes & development*.  
914 1993;7(5):812-21.
- 915 51. Matsushime H, Roussel MF, Ashmun RA, Sherr CJ. Colony-stimulating factor 1  
916 regulates novel cyclins during the G1 phase of the cell cycle. *Cell*.  
917 1991;65(4):701-13.
- 918 52. Dulic V, Lees E, Reed SI. Association of human cyclin E with a periodic G1-S  
919 phase protein kinase. *Science*. 1992;257(5078):1958-61.

- 920 53. Koff A, Giordano A, Desai D, Yamashita K, Harper JW, Elledge S, et al.  
921 Formation and activation of a cyclin E-cdk2 complex during the G1 phase of the  
922 human cell cycle. *Science*. 1992;257(5077):1689-94.
- 923 54. Taylor EW. The Mechanism of Colchicine Inhibition of Mitosis. I. Kinetics of  
924 Inhibition and the Binding of H3-Colchicine. *The Journal of cell biology*.  
925 1965;25:SUPPL:145-60.
- 926 55. Hervás JP, Fernández-Gómez ME, Giménez-Martín G. Colchicine Effect on the  
927 Mitotic Spindle: Estimate of Multipolar Anaphase Production. *Caryologia*.  
928 1974;27(3):359-68.
- 929 56. Rieder CL, Palazzo RE. Colcemid and the mitotic cycle. *Journal of cell science*.  
930 1992;102 ( Pt 3):387-92.
- 931 57. Baumann DG, Gilmour DS. A sequence-specific core promoter-binding  
932 transcription factor recruits TRF2 to coordinately transcribe ribosomal protein  
933 genes. *Nucleic acids research*. 2017;45(18):10481-91.
- 934 58. Baumann DG, Dai MS, Lu H, Gilmour DS. GFZF, a glutathione S-transferase  
935 protein implicated in cell cycle regulation and hybrid inviability, is a transcriptional  
936 co-activator. *Molecular and cellular biology*. 2017.
- 937 59. Bailey TL, Boden M, Buske FA, Frith M, Grant CE, Clementi L, et al. MEME  
938 SUITE: tools for motif discovery and searching. *Nucleic acids research*.  
939 2009;37(Web Server issue):W202-8.
- 940 60. Ohler U, Liao GC, Niemann H, Rubin GM. Computational analysis of core  
941 promoters in the *Drosophila* genome. *Genome Biol*.  
942 2002;3(12):RESEARCH0087.
- 943 61. Sloutskin A, Danino YM, Orenstein Y, Zehavi Y, Doniger T, Shamir R, et al.  
944 ElemeNT: a computational tool for detecting core promoter elements.  
945 *Transcription*. 2015;6(3):41-50.
- 946 62. Li J, Gilmour DS. Distinct mechanisms of transcriptional pausing orchestrated by  
947 GAGA factor and M1BP, a novel transcription factor. *The EMBO journal*.  
948 2013;32(13):1829-41.
- 949 63. Maeda R, Tamashiro H, Takano K, Takahashi H, Suzuki H, Saito S, et al. TBP-  
950 like Protein (TLP) Disrupts the p53-MDM2 Interaction and Induces Long-lasting  
951 p53 Activation. *The Journal of biological chemistry*. 2017;292(8):3201-12.
- 952 64. Akdemir F, Christich A, Sogame N, Chapo J, Abrams JM. p53 directs focused  
953 genomic responses in *Drosophila*. *Oncogene*. 2007;26(36):5184-93.
- 954 65. Brodsky MH, Weinert BT, Tsang G, Rong YS, McGinnis NM, Golic KG, et al.  
955 *Drosophila melanogaster* MNK/Chk2 and p53 regulate multiple DNA repair and  
956 apoptotic pathways following DNA damage. *Molecular and cellular biology*.  
957 2004;24(3):1219-31.
- 958 66. Zhang Y, Lin N, Carroll PM, Chan G, Guan B, Xiao H, et al. Epigenetic blocking  
959 of an enhancer region controls irradiation-induced proapoptotic gene expression  
960 in *Drosophila* embryos. *Developmental cell*. 2008;14(4):481-93.
- 961 67. Chakraborty R, Li Y, Zhou L, Golic KG. Corp Regulates P53 in *Drosophila*  
962 *melanogaster* via a Negative Feedback Loop. *PLoS Genet*.  
963 2015;11(7):e1005400.
- 964 68. Isogai Y, Keles S, Prestel M, Hochheimer A, Tjian R. Transcription of histone  
965 gene cluster by differential core-promoter factors. *Genes & development*.  
966 2007;21(22):2936-49.
- 967 69. Kedmi A, Zehavi Y, Glick Y, Orenstein Y, Ideses D, Wachtel C, et al. *Drosophila*  
968 TRF2 is a preferential core promoter regulator. *Genes & development*.  
969 2014;28(19):2163-74.

- 970 70. McCleland ML, O'Farrell PH. RNAi of mitotic cyclins in *Drosophila* uncouples the  
971 nuclear and centrosome cycle. *Current biology : CB*. 2008;18(4):245-54.  
972 71. Yuan K, O'Farrell PH. Cyclin B3 is a mitotic cyclin that promotes the metaphase-  
973 anaphase transition. *Current biology : CB*. 2015;25(6):811-6.  
974 72. Teves SS, An L, Bhargava-Shah A, Xie L, Darzacq X, Tjian R. A stable mode of  
975 bookmarking by TBP recruits RNA polymerase II to mitotic chromosomes. *eLife*.  
976 2018;7:e35621.  
977 73. Richardson H, O'Keefe LV, Marty T, Saint R. Ectopic cyclin E expression  
978 induces premature entry into S phase and disrupts pattern formation in the  
979 *Drosophila* eye imaginal disc. *Development*. 1995;121(10):3371-9.  
980 74. Anders S, Pyl PT, Huber W. HTSeq--a Python framework to work with high-  
981 throughput sequencing data. *Bioinformatics*. 2015;31(2):166-9.  
982 75. Love MI, Huber W, Anders S. Moderated estimation of fold change and  
983 dispersion for RNA-seq data with DESeq2. *Genome Biol*. 2014;15(12):550.  
984 76. Szklarczyk D, Gable AL, Lyon D, Junge A, Wyder S, Huerta-Cepas J, et al.  
985 STRING v11: protein-protein association networks with increased coverage,  
986 supporting functional discovery in genome-wide experimental datasets. *Nucleic  
987 acids research*. 2019;47(D1):D607-D13.  
988 77. Peng Q, Wang Y, Li M, Yuan D, Xu M, Li C, et al. cGMP-Dependent Protein  
989 Kinase Encoded by foraging Regulates Motor Axon Guidance in *Drosophila* by  
990 Suppressing Lola Function. *J Neurosci*. 2016;36(16):4635-46.  
991 78. George TC, Fanning SL, Fitzgerald-Bocarsly P, Medeiros RB, Highfill S, Shimizu  
992 Y, et al. Quantitative measurement of nuclear translocation events using  
993 similarity analysis of multispectral cellular images obtained in flow. *J Immunol  
994 Methods*. 2006;311(1-2):117-29.  
995 79. Hendzel MJ, Wei Y, Mancini MA, Van Hooser A, Ranalli T, Brinkley BR, et al.  
996 Mitosis-specific phosphorylation of histone H3 initiates primarily within  
997 pericentromeric heterochromatin during G2 and spreads in an ordered fashion  
998 coincident with mitotic chromosome condensation. *Chromosoma*.  
999 1997;106(6):348-60.  
1000 80. Filby A, Perucha E, Summers H, Rees P, Chana P, Heck S, et al. An imaging  
1001 flow cytometric method for measuring cell division history and molecular  
1002 symmetry during mitosis. *Cytometry A*. 2011;79(7):496-506.  
1003

1004 **Figure Legends**

1005 **Fig. 1.**

1006 *Trf2* Knockdown enhances early and late apoptosis in S2R+ cells. *Drosophila* S2R+  
1007 cells were incubated for three days with dsRNA directed against *Trf2*, *exd*, *Tbp* and  
1008 *Trf1*. To examine whether *Trf2* knockdown triggers apoptotic cell death, cells were  
1009 harvested following 72 h and stained with Annexin-V FITC and PI. **a** FACS analysis  
1010 of a representative experiment. **b** Average percentages of cells undergoing early and  
1011 late apoptosis. (n=4, \*0.01 < p ≤ 0.05, \*\*0.005 ≤ p ≤ 0.01, \*\*\*p < 0.005, two-tailed  
1012 Students t-test; comparison to mock).

1013

1014 **Fig. 2.**

1015 The expression levels of distinct pro-apoptotic genes increase following knockdown  
1016 of TRF2. *Drosophila* S2R+ cells were incubated for three days with dsRNA directed  
1017 against TRF2, *exd*, TBP and TRF1. RNA was isolated from the cells and reverse  
1018 transcribed to cDNA. qPCR experiments were used to analyze the RNA levels of the  
1019 endogenous genes: **a** *Trf2*, *TBP*, *TRF1*, *rpr*, *hid*, *grim*, *scyl*, *Buffy*, *Debcl* and *Dronc*  
1020 and **b** *Trf2*, *p53* and *TBP*. qPCR experiments were performed in triplicates, and the  
1021 graph represents the average of three to eight experiments. Error bars represent the  
1022 SEM. \*p< 0.05, one-way ANOVA followed by Tukey's post hoc test as compared to  
1023 the mock treatment of the relevant gene.

1024

1025 **Fig. 3.**

1026 *Trf2*, but not *Tbp* or *Trf1* knockdown, affects cell cycle distribution. *Drosophila* S2R+  
1027 cells were incubated for three days with dsRNA directed against *Trf2*, *Tbp*, *Trf1* and  
1028 *exd*. Cells were fixed with 80% ethanol and stained with Propidium-Iodide (PI) for

1029 flow cytometry (FACS) analysis. **a** Cell cycle distribution histograms of a  
1030 representative experiment. **b** Average cell cycle distribution determined by FACS  
1031 analyses of eight independent experiments (\* $0.01 < p \leq 0.05$ , \*\* $0.005 \leq p \leq 0.01$ , \*\*\* $p$   
1032  $< 0.005$ , two-tailed Students t-test; comparison to mock).

1033

1034 **Fig. 4.**

1035 TRF2 is involved in S phase progression. *Drosophila* S2R+ cells were incubated for  
1036 three days with dsRNA probes directed against *Trf2* or *Tbp*. Next, cells were either  
1037 left untreated or treated with 1mM Hydroxyurea for 18h. The cells were allowed to  
1038 resume cell cycle for 2h, 4h, 6h or 8h in fresh medium containing 40µM 5-Bromo-2'-  
1039 deoxyuridine (BrdU), and were then fixed with 80% ethanol overnight and analyzed  
1040 by FACS using BrdU-PI staining. Each histogram plots the PI fluorescence intensity  
1041 (representing DNA content) on the X-axis, and cell count on the Y-axis.

1042

1043

1044 **Fig. 5.**

1045 Knock down of *Trf2* expression by RNAi reduces the expression of cyclin genes.  
1046 *Drosophila* S2R+ cells were incubated for three days with dsRNA probes directed  
1047 against *Trf2*, *exd*, *Tbp* and *Trf1*. RNA was isolated from the cells and reverse  
1048 transcribed (RT) to cDNA. Real-time PCR (qPCR) experiments were used to analyze  
1049 the RNA levels of the endogenous genes: **a** *Trf2*, CycA, CycB, CycB3, CycC, CycD  
1050 and **b** CycE. As there were differences in CycE expression following RNAi with  
1051 probe #1 compared to probe #2, four non-overlapping probes were used to  
1052 knockdown *Trf2* expression towards the analysis of CycE expression. qPCR  
1053 experiments were performed in triplicates, and the graph represents the average of

1054 three to eight experiments. Error bars represent the SEM. \* $p < 0.05$ , one-way  
1055 ANOVA followed by Tukey's post hoc test as compared to the mock treatment of the  
1056 relevant gene. **c** Western blot analysis following TRF2 and TBP knockdown in S2R+  
1057 cells, using anti-TRF2 polyclonal antibodies and anti-Cyc E monoclonal antibodies.  
1058 Actin was used as a loading control.

1059

1060 **Fig. 6.**

1061 TRF2 regulates cell cycle progression through mitosis. *Drosophila* S2R+ cells were  
1062 incubated for three days with dsRNA directed against TRF2 or TBP. Cells were then  
1063 fixed with 4% PFA and stained with a phospho-Histone H3 (Ser10) antibody (PH3,  
1064 mitotic marker; green), Hoechst (DNA visualization; Blue) and Phalloidin (filamentous  
1065 Actin visualization; red). **a** Representative confocal microscopy images of *Drosophila*  
1066 S2R+ cells in different mitotic phases. **b** Comparison of mitotic indices following each  
1067 treatment, calculated based on microscopic analysis. Shown are the averages of  
1068 three independent experiments, in which a total of 100,000-800,000 cells were  
1069 analyzed for each treatment (\* $0.01 < p \leq 0.05$ , \*\* $0.005 \leq p \leq 0.01$ , \*\*\* $p < 0.005$ , two-  
1070 tailed Students t-test; comparison to mock). **c** Representative images obtained by  
1071 imaging flow cytometry analysis. **d** Comparison of mitotic indices following each  
1072 treatment, calculated based on imaging flow cytometry. Shown are the averages of  
1073 three independent experiments, in which a total of 40,000 cells were analyzed for  
1074 each treatment (\* $0.01 < p \leq 0.05$ , \*\* $0.005 \leq p \leq 0.01$ , \*\*\* $p < 0.005$ , two-tailed  
1075 Students t-test; comparison to mock). **e-f** Distribution of mitotic phases among all  
1076 mitotic cells, based on imaging flow cytometry. Shown are the averages of three  
1077 independent experiments, in which a total of 40,000 cells were analyzed for each  
1078 treatment (\* $0.01 < p \leq 0.05$ , \*\* $0.005 \leq p \leq 0.01$ , \*\*\* $p < 0.005$ , two-tailed Students t-

1079 test; comparison to mock). Filled triangles indicate aberrant chromosomal  
1080 morphology in Colchicine-treated cells. Phospho-Histone H3 Ser10-positive cells (**e**),  
1081 were analyzed separately from the Phospho-Histone H3 Ser10-negative cells  
1082 undergoing mitosis (**f**). Phospho-Histone H3 Ser10-negative cells undergoing mitosis  
1083 (as identified by the imaging flow cytometer) were defined as cells in telophase (**f**).  
1084 Notably, cell counts of telophase cells likely include Phospho-Histone H3 Ser10-  
1085 negative doublet cells, which, even using the high-resolution Imagestream, could not  
1086 be distinguished from telophase cells.

1087  
1088 **Fig. 7.**

1089 CycA and CycB expression is affected by TRF2 knockdown, and less by GFZF and  
1090 M1BP. **a** Schematic representation of genes containing at least one binding site of  
1091 the specified transcription factor at  $\pm 50$ bp relative to its TSS, as determined by  
1092 FlyBase. ChIP-exo data was retrieved from GSE97841 and GSE105009. **b** Top  
1093 enriched motif among the 4331 commonly bound promoters, as detected by MEME  
1094 analysis. Its resemblance to Ohler Motif 1 is depicted by the motif logo derived by  
1095 M1BP ChIP-exo (57). **c** The 4331 commonly bound regions were analyzed for core  
1096 promoter composition. This promoter group was found to be depleted for the TATA-  
1097 box motif and enriched for dTCT and the Motif 1 core promoter elements. p-values  
1098 were adjusted using Bonferroni correction. \*\*\* $p < 10^{-5}$ . **d-e** *Drosophila* S2R+ cells  
1099 were incubated for three days with dsRNA probes directed against *Trf2* (probe #1),  
1100 *gfzf*, *M1BP* or their combinations. RNA was isolated from the cells and reverse  
1101 transcribed (RT) to cDNA. Real-time PCR (qPCR) experiments were used to analyze  
1102 the RNA levels of the endogenous of *Trf2*, *gfzf* and *M1BP*, as well as *CycA*, *CycB*,  
1103 *CycD* and *CycE* genes, as indicated. **d** Single knockdowns of *Trf2*, *gfzf* or *M1BP*. **e**  
1104 Knockdown of multiple genes, as indicated. qPCR experiments were performed in

1105 triplicates, and the graph represents the average of 4 independent experiments.  
1106 Error bars represent the SEM. \* $p < 0.05$ , one-way ANOVA followed by Tukey's post  
1107 hoc test as compared to the mock treatment of the relevant gene.

1108

1109

1110 **Additional files**

1111 **Additional file 1: Figure S1. .pdf**

1112 A) Schematic representation of dsRNA TRF2 probes used in this study. B) Western  
1113 blot analysis following TRF2 and C) TBP knockdown in S2R+ cells, using anti-TRF2  
1114 and anti-TBP polyclonal antibodies, respectively. Actin and  $\gamma$ -Tubulin were used as  
1115 loading controls.

1116 **Additional file 2: Table S1. .xlsx**

1117 GO terms analysis of the RNA-seq data. Summary, as well as the exact GO terms  
1118 are provided, according to the datasheet name. Analysis was performed sing  
1119 STRING. Only genes with pAdj <0.1 were considered. DEseq2 output is presented  
1120 for either *Trf2* or *Tbp* knockdown, as compared to mock at 72h post silencing.

1121

1122 **Additional file 3: Figure S2. .pdf**

1123 TBP overexpression does not result in induction of pro-apoptotic gene expression.  
1124 *Drosophila* S2R+ cells were depleted of *Trf2* by RNAi and then transfected with  
1125 either pAc-empty (mock) or TBP expression vector. Cells were harvested 36–48h  
1126 following transfection, RNA was purified and reverse transcribed to cDNA for RT-  
1127 qPCR analysis. qPCR experiments were performed in triplicates, and the graph  
1128 represents the average of 3 experiments. Error bars represent the SEM. \* $p < 0.05$ ,

1129 two-tailed Students t-test; comparison to the same treatment without TBP  
1130 overexpression.

1131

1132 **Additional file 4: Figure S3. .pdf**

1133 TRF2 is involved in S phase progression. *Drosophila* S2R+ cells were incubated for  
1134 three days with dsRNA probes directed against *Trf2* or *Tbp*. Next, cells were either  
1135 left untreated or treated with 1mM Hydroxyurea for 18h. The cells were allowed to  
1136 resume cell cycle for 2h, 4h, 6h or 8h in fresh medium containing 40µM BrdU, and  
1137 were then fixed with 80% ethanol overnight and analyzed by FACS using BrdU-PI  
1138 staining. The PI fluorescence intensity (representing DNA content) is plotted on the  
1139 X-axis (linear scale), and the BrdU-FITC fluorescence intensity (representing BrdU  
1140 incorporation into the DNA) is plotted on the Y-axis (log scale).

1141

1142 **Additional file 5: Figure S4. .pdf**

1143 Gating and masking strategy for imaging-flow cytometry data analysis. *A*) Cells were  
1144 gated for single cells, using the area and aspect ratio features on the BF image. *B*)  
1145 Centered and uncropped cells were gated based on the centroid X (the number of  
1146 pixels in the horizontal axis from the upper left corner of the image to the center of  
1147 the mask) and area features. *C*) Focused cells were gated, using the Gradient RMS  
1148 feature, as previously described (78). *D*) The G2/M population was gated out of the  
1149 focused cells, based on DNA (Hoechst) intensity. *E*) Mitotic cells were gated from the  
1150 G2M population, as the high intensity population of pH3 staining, based on the  
1151 intensity feature of pH3 and Max pixel feature of pH3 (the largest value of the  
1152 background-subtracted pixels contained in the input mask). *F*) To include only single  
1153 positive pH3 stained cells, doublet cells were eliminated by gating the single cells

1154 from the mitotic population, using the area and aspect ratio features of the BF. G) To  
1155 discriminate between the different mitotic phases subpopulations, several masks  
1156 were created: 1. A morphology mask that includes all pixels within the outermost  
1157 image contour. 2. A threshold mask that includes the highest intensity pixels  
1158 (indicated as percentages). 3. A range mask that selects components in an image  
1159 within a selected size ( $\mu\text{m}$ ), was used to eliminate small components.  
1160 Furthermore, the following features were used on the combined masks:  
1161 1. Spot count - the number of connected components in an image.  
1162 2. Aspect ratio intensity - the aspect ratio weighted for fluorescence intensity.  
1163 These masks were combined and the features were calculated and plotted as  
1164 follows:  
1165 Spot count of the combined mask: range (threshold 75%, M07) 20-5000, was plotted  
1166 against the aspect ratio intensity of the combined mask: range  
1167 (Threshold(Morphology(M07), 82%) 15-5000.  
1168 The prophase population was defined as having a more circular nuclear staining  
1169 (aspect ratio intensity should be high), and was hence gated as one nuclear spot  
1170 count with aspect ratio intensity bigger than 0.6. On the other hand, the metaphase  
1171 population was defined as having a more elongated DNA distribution and was gated  
1172 as one nuclear spot count with aspect ratio intensity smaller than 0.6. Finally, the  
1173 anaphase population was gated as cells with two nuclear spots having aspect ratio  
1174 intensity less than 0.6. (80). H) As serine 10 of histone H3 becomes  
1175 dephosphorylated during telophase, the telophase population was derived from the  
1176 negative pH3-stained cells. To identify telophase pairs, an object mask was created  
1177 (which segments images to closely identify the area corresponding to the cell). The  
1178 circularity feature (which measures the degree of the mask's deviation from a circle)

1179 of the object mask (BF), was plotted against the aspect ratio intensity of the M07  
1180 DNA mask. Telophase cells were gated as having the lowest BF circularity and as  
1181 the most elongated, based on DNA stain (lowest aspect ratio intensity (M07)).

1182

1183 **Additional file 6: Table S2. .doc**

1184 Number of cells in each mitotic phase within phospho-Histone H3 Ser10-positive  
1185 mitotic cells or telophase.

1186

1187 **Additional file 7: Figure S5. .pdf**

1188 *Drosophila* S2R+ cells treated with Colchicine display aberrant chromosomal  
1189 morphology. Colchicine-treated cells were fixed with 4% PFA and stained with a  
1190 phospho-Histone H3 (Ser10) antibody (green), Hoechst (DNA visualization; blue)  
1191 and Acti-stain 670 Phalloidin (filamentous Actin visualization; red). A) Shown are  
1192 representative images of cells in different mitotic phases obtained by imaging flow  
1193 cytometry analysis. B) Quantitation of cells with aberrant DNA morphology within  
1194 mock and colchicine-treated cells using imaging flow cytometry analysis. Prophase-  
1195 and metaphase-gated cells within either mock or colchicine-treated S2R+ cells, were  
1196 further gated using calculations of the following features:

1197 1. The Delta centroid XY feature (which measures the distance in microns between  
1198 the centroid feature of two images using the user provided masks) was calculated  
1199 using the BF default mask and Hoechst channel mask of the 60% most highly  
1200 intense pixels. Cells with centered nucleus will get a lower value while polar located  
1201 nucleus will get a higher value. 2. The Max contour position feature (the location of  
1202 the contour in the cell that has the highest intensity concentration; the score is  
1203 between 0 to 1, with 0 being the object center and 1 the object perimeter). To

1204 distinguish between central vs. polar location of the dividing nucleus, the Delta-  
1205 centroid XY was plotted against the Max contour position, and polar DNA was gated  
1206 as having the highest values of both features. Depicted are the analyses of cells in  
1207 prophase and metaphase. Cells in anaphase are not shown due to the low number  
1208 of cells observed in anaphase (Additional file 6).

1209

1210 **Additional file 8: Table S3. .xlsx**

1211 Mass-spectrometry data for short TRF2, long TRF2 and TBP proteins.

1212

1213 **Additional file 9: Figure S6. .pdf**

1214 Knockdown of *M1BP* specifically elevates the expression of *CycA* and ribosomal  
1215 protein genes. *Drosophila* S2R+ cells were incubated for three days with dsRNA  
1216 probes as indicated in the legend. RNA was isolated from the cells and reverse  
1217 transcribed (RT) to cDNA. Real-time PCR (qPCR) experiments were used to analyze  
1218 the RNA levels of the endogenous genes. qPCR experiments were performed in  
1219 triplicates, and the graph represents the average of 3 experiments  $\pm$  SEM. A) *CycA*  
1220 expression levels are reduced following *Trf2* knockdown, but not *gfzf* or *M1BP*  
1221 knockdown. \* $p < 0.05$ , one-way ANOVA followed by Tukey's post hoc test as  
1222 compared to the mock treatment of the relevant gene. B) Additional ribosomal genes  
1223 are influenced by *M1BP* knockdown, however not all genes are upregulated in  
1224 response to *M1BP* knockdown. *CG12493* and *sgll* genes were previously shown to  
1225 be downregulated upon *M1BP* knockdown (62). \*\* $p < 0.01$ , two-tailed Students t-test;  
1226 compared to mock treatment.

1227

**Table 1.**

Primers for generation of dsRNA probes

dsRNA probe	Forward primer	Reverse primer
Trf2 #1	ATAGGTACCGGCAACCGGCAGTAAAAATA	ATAACTAGTACTCCACATTGATCCCTGC
Trf2 #2	ATACTCGAGAACAGAAGGAGCAGCATCGT	ATAACTAGTTATTTTACTGCCGGTTGCC
Trf2 #3	ATAGGTACCAAGGAGAACCAATGCCGAAT	ATAACTAGTATTAGAAGAACTTAAGCGATC
Trf2 #4	ATACTCGAGCAATCTGACTTGAATCCGG	ATAACTAGTTCATCTGAAGCTTGTGCG
exd	ATAACTAGTCGATGGTGCTGACAATGCC	ATAGGTACCGGGGCTTAGATCCTGATGGAG
Trf1	GGGGTACCGGACAGGGATAATGTGGCTG	AAAATAGTGGCTTGACCATGCGATAGAT
Tbp	GGGGTACCACATGATGCCCATGAGTGA	AAAATAGTAATGGGAATATCTTGTGAG
rpr	AAGGTACCACGAAAGAAAAGTGTGCG	AAAATAGTTGCAATTAGCCAACCTCG
scyl	AAGGTACCTACTACGCTGCTGACGAGGA	AAAATAGTATCACCATTAGTTGGTGGCG
p53	AAGGTACCGATGCTGCAGGACATTAGA	AAAATAGTCTGGCTATCATTGCTCTCC
M1BP	GGGGTACCATATTAACACGAAACACCAGG	AAAATAGTACCTTGGTGTGTCGATCTC
gfzf	GGGGTACCTCAGCATCTGTTCCACTTCG	AAAATAGTGTGTGAATGTGGTCGAG

**Table 2.**

Real-time PCR (qPCR) primers

Gene	Forward primer	Reverse primer
<i>Gapdh2</i>	TTCCCTCAGCGACACCCACTC	ATGACGCCGGTTGGAGTAGCC
<i>Trf2</i>	GGAATCGTCTTCTGGGGACT	GACGACTCCTGTTGGCTTG
<i>CycA</i>	TGGGCACGGCAGCTATGTAT	CCTGCGCCTGGTGTAACTG
<i>CycB</i>	CGAGCACCATACGATGTCCA	TTGAGCAAGTGCAGCGACAG
<i>CycB3</i>	TCCCAGAGACTGCTCCAAGC	CATGGCGTAGTGGGACACCT
<i>CycC</i>	CACCGATGTCTGCCTGCTC	GCACGATCTCCTGGACCTTG
<i>CycD</i>	AGGTGAGGAGAACGACACCAC	CCTCGGCACACACTTCCAT
<i>CycE</i>	CTCGGTTTGAGCCTCCATC	AGACAACGGGCGAGGTGTAG
<i>Tbp</i>	TCAGCTCCGGCAAGATGGTG	GCAGGGAAACCGAGCTTTGG
<i>Trf1</i>	AGAAGCTGGATTCCCCGTA	GCACGTGGTTGAGGTTCTCC
<i>exd</i>	GCGAAATCAAGGAGAACGACCGTCC	CCTCGGCAATCAGCATGTTGTCC
<i>rpr</i>	CATAACCGATCAGGCGACTC	GTGTACTGGCGCAGGGTTTC
<i>hid</i>	CGACCTCCACGCCGTTATC	GCTCTGGTACTCGCGCTCAT
<i>grim</i>	TTTGGCCCAGATCTTCTGCT	GCATCAGTCACGTCGTCTC
<i>Debcl</i>	ACAGCATGGCGAGGAACCT	ATGTCGCTGTCCTCCAGCTC
<i>scyl</i>	ATAATCCCGGTGTCGGAGAA	CCGTATCCGAATCGACCTTG
<i>buffy</i>	TTCTCAGGGTCGTTGCCTGT	TGGAGGTGGAGCCCAGTATG
<i>p53</i>	TTAGCGTTGAGCCTTGACG	CAGGGGGACTACAACGGAAA
<i>M1BP</i>	AATTGGCTGCGAACTCTGT	CAGCGGCCACAGTACTTACA
<i>gfzf</i>	GAACCCACCGGATATGTCAC	TGCTGGCAGGGCTTAAGTT
<i>RpLP2</i>	GACATGGCTTCGCTCTCTT	GTGAACGGATGGGTGCTACA
<i>RpS12</i>	CAAGCGTCAGGCTGTTCTGT	CAGCTTCTGTGCGAGTCCA
<i>CG12493</i>	GACAACCAATTGGATCAGGAAAG	AGATTACCATCGGGCATATT
<i>sgll</i>	ATTGAAAGGATGAGCCAAGG	CCAGTCTCGGAATACACAGAAG
<i>RpL30</i>	CAAATACTGCCTGGCTACA	TACTCGATCTCGGACTTCCTC
<i>RpLP1</i>	CACTTCGACATGTCCACCAA	CCTTCAGGATGGTGTGATCTT

**Table 3.**

Enrichment of TRF2, TBP, M1BP and GFZF in FLAG-immuno-affinity purified complexes from inducible S2R+ cells

Name of purified (/co-purified) protein	Enrichment of purified (/co-purified) proteins within		
	Short TRF2-associated proteins	Long TRF2-associated proteins	TBP-associated proteins
TRF2	78.695	6.128	-
TBP	-	-	18.3
M1BP	1.795E7	-	-
GFZF	1.683E7	-	-

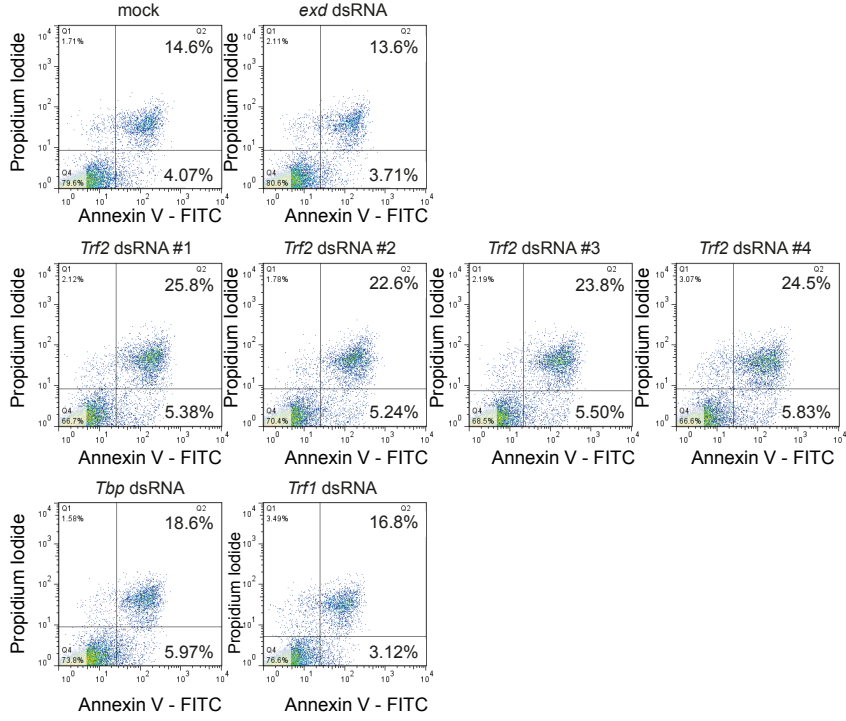
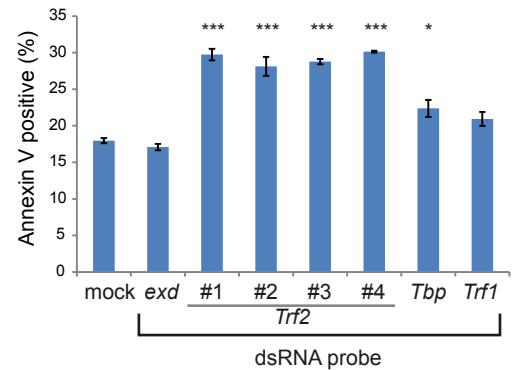
The values in the table represent the enrichment of each purified (/co-purified) protein in the indicated sample. The enrichment was calculated as the ratio between the mass spectrometry area (the average of the three most intense peptides from each protein) of the induced sample and the un-induced sample.

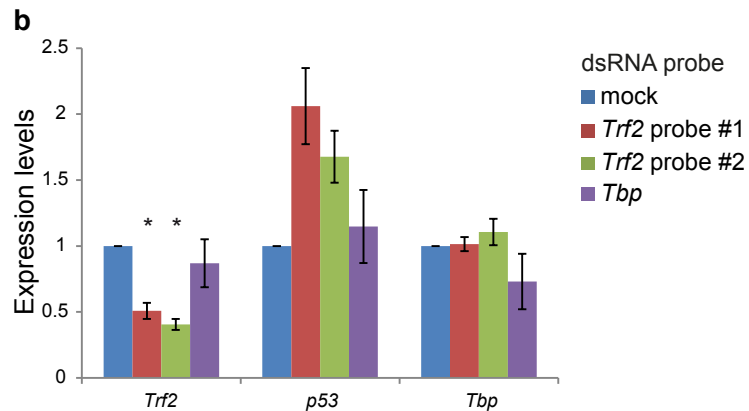
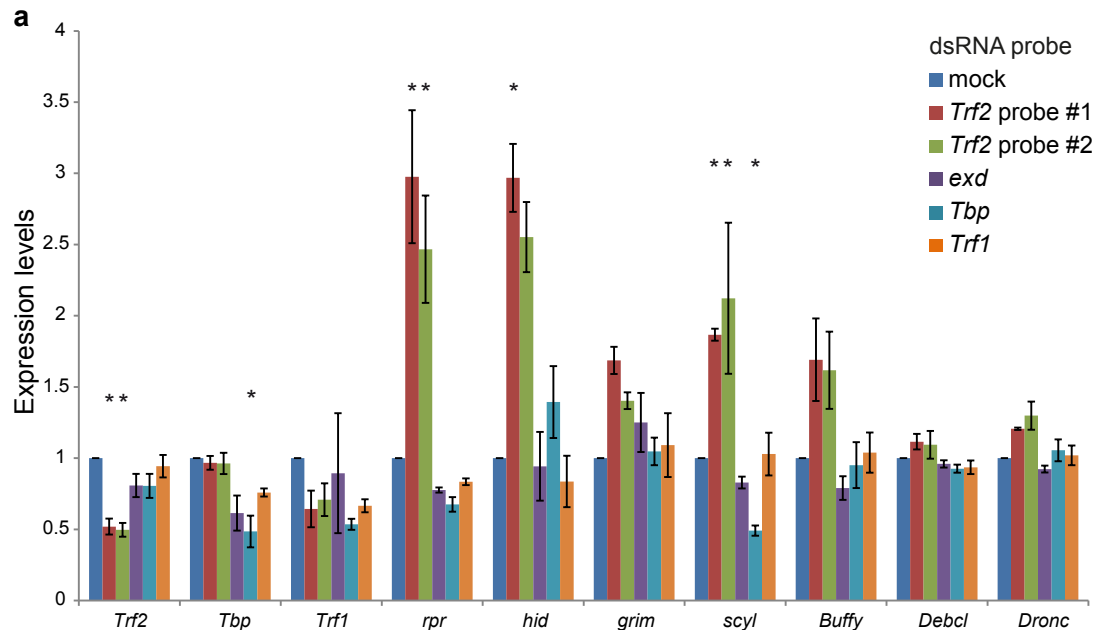
**Table 4.**

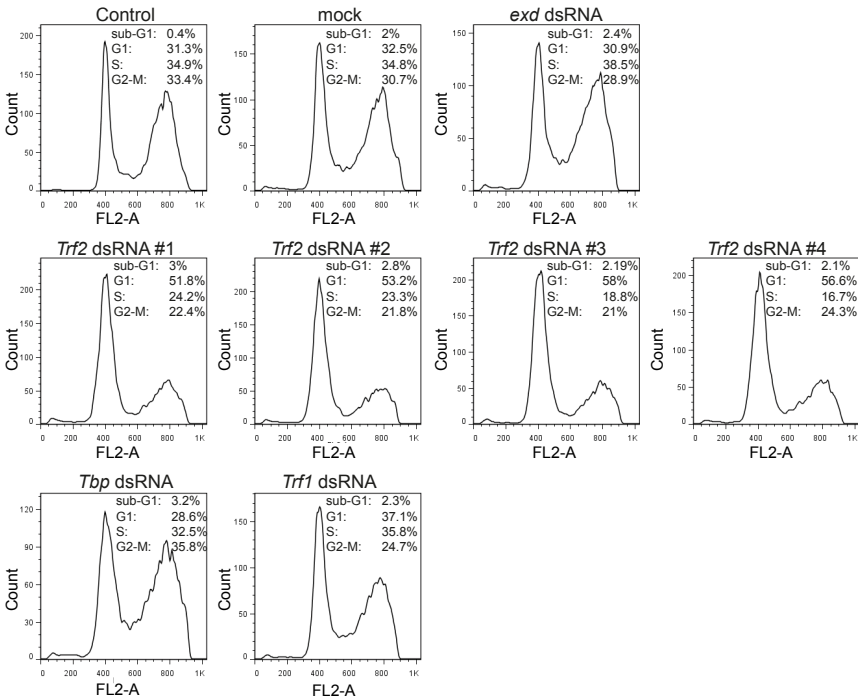
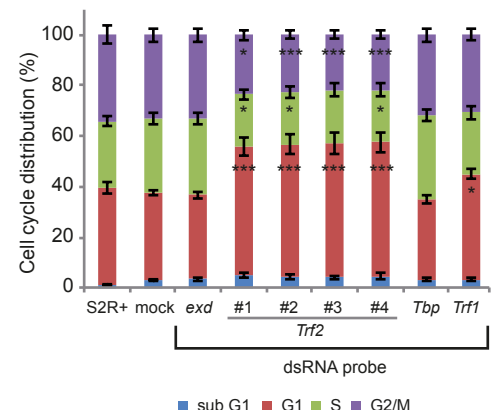
TRF2, M1BP and GFZF occupancy within -100 to +100 relative to the TSSs

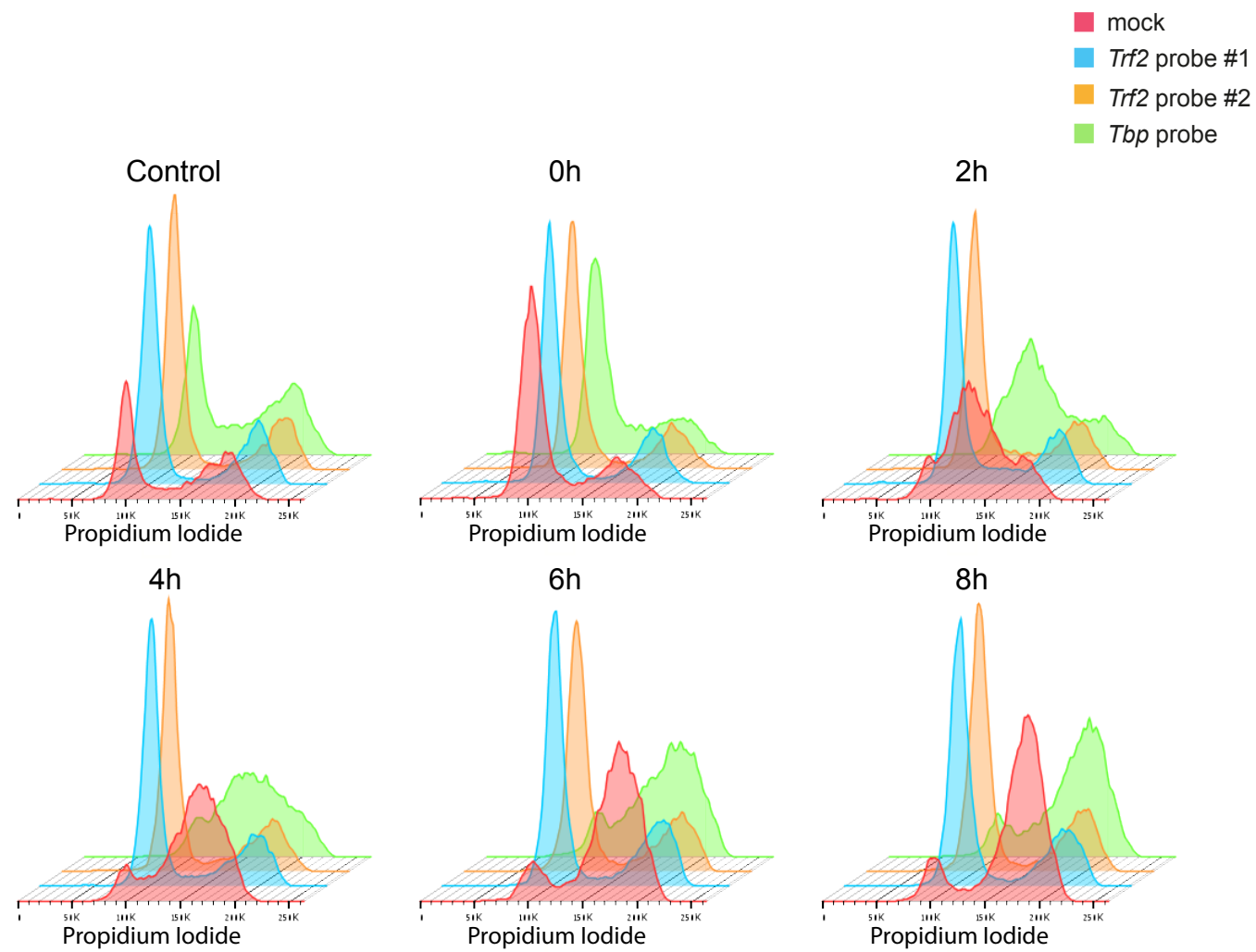
Gene name	TSS Location	TRF2			M1BP			GFZF		
		# of bound sites	Max. peak score	Avg. peak score	# of bound sites	Max. peak score	Avg. peak score	# of bound sites	Max. peak score	Avg. peak score
CycA_1	chr3L:11826617	1	54.16	54.16	59	126.93	30	2	112.85	87.78
CycA_2	chr3L:11826310	1	36.11	36.11	1	20.04	20.04	0	0	0
CycB_1	chr2R:18694432	15	150.45	38.11	47	106.89	26.72	3	114.64	62.1
CycB_2	chr2R:18694437	15	150.45	38.11	51	106.89	25.28	3	114.64	62.1
CycB_3	chr2R:18694449	15	150.45	38.11	60	106.89	27.28	3	114.64	62.1
CycB3	chr3R:20696533	4	90.27	40.62	128	140.29	36.69	9	157.63	72.05
CycE_1	chr2L:15746609	2	66.2	42.13	1	6.68	6.68	0	0	0
CycE_2	chr2L:15748123	4	60.18	31.6	8	53.44	30.9	1	136.14	136.14
CycC_1	chr3R:10715915	4	36.11	24.07	4	66.81	23.38	1	42.99	42.99
CycC_2	chr3R:10715922	4	36.11	24.07	3	66.81	26.72	1	42.99	42.99
CycD_1	chrX:15803691	2	42.13	24.08	7	46.76	20.04	0	0	0
CycD_2	chrX:15803682	2	42.13	24.08	7	46.76	20.04	0	0	0
RpL5	chr2L:22429377	74	210.63	51.56	142	140.29	33.07	29	148.68	48.36
RpL7	chr2L:10201108	23	210.63	50.50	121	374.11	62.44	5	118.23	65.92
RpL23	chr2R:18741912	38	132.4	46.25	200	327.35	51.27	68	449.61	99.00
RpL30	chr2L:19009229	21	102.31	30.38	141	233.82	47.81	16	231.08	76.58
RpLP1	chr2L:419957	14	156.47	44.28	148	180.38	37.78	19	195.25	74.10
RpLP2	chr2R:12473638	48	234.71	67.08	175	173.70	37.37	8	175.55	65.16

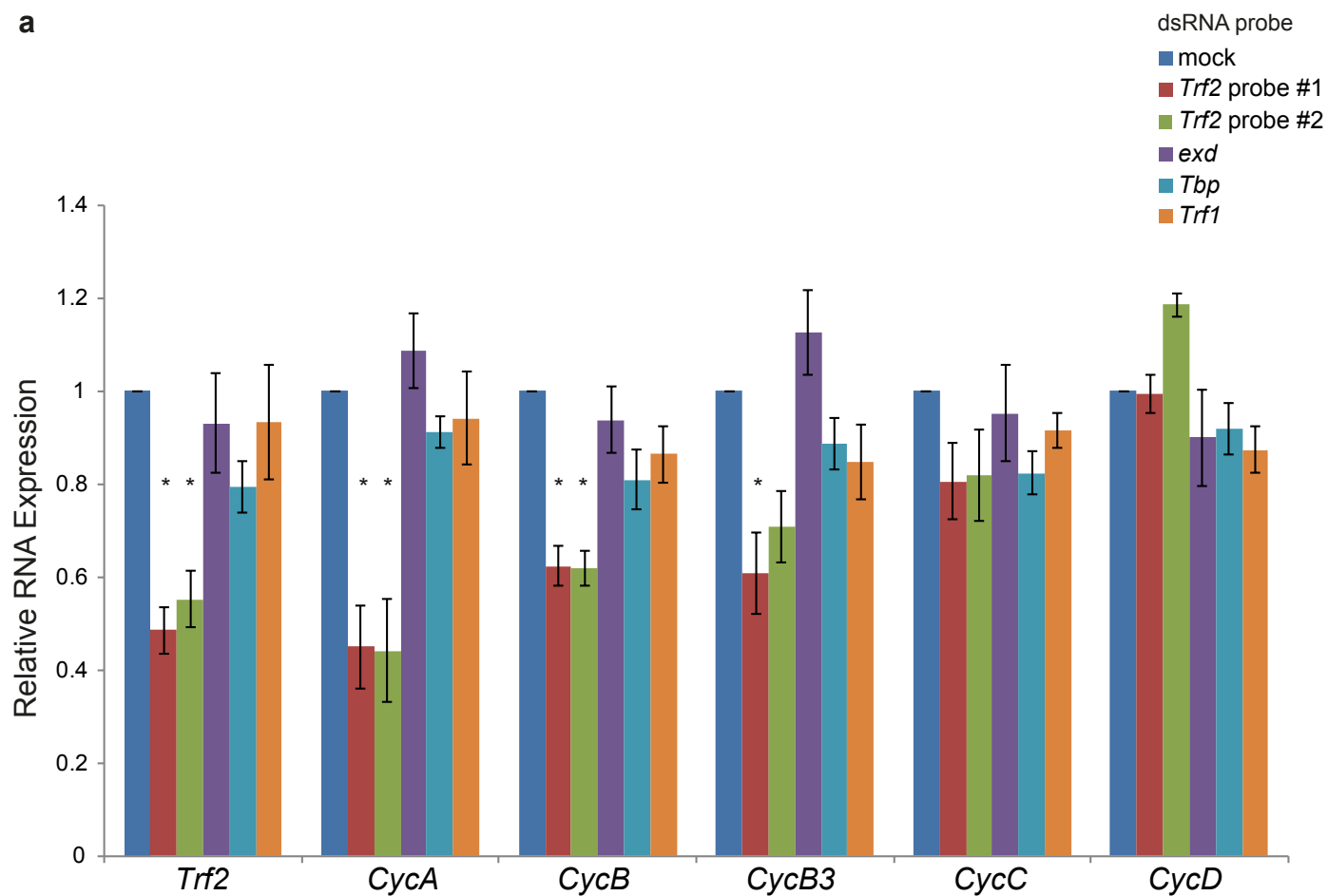
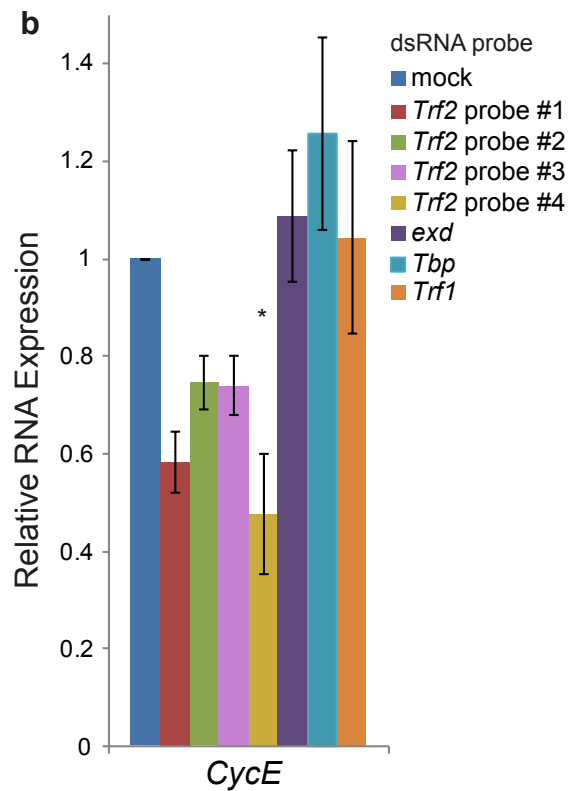
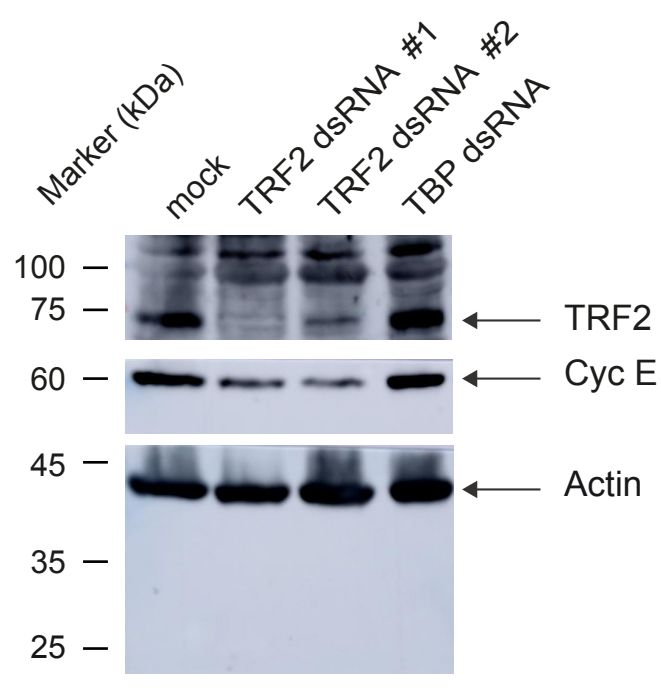
TRF2, M1BP and GFZF occupancy data (number of bound sites, the maximum peak scores and the average peak scores) was retrieved from ChIP-exo experiments performed in *Drosophila* S2R+ cells (GSE97841 and GSE105009) (64, 65). Due to variations in TSSs obtained by different methods, we relate to -100 to +100 relative to the TSSs peaks from available 5'GRO-seq and focused TSS analysis in S2 cells (GSE68677 and <http://labs.biology.ucsd.edu/Kadonaga/drosophila.tss.data/>) and PRO-cap analysis in S2 cells (GSM1032759).

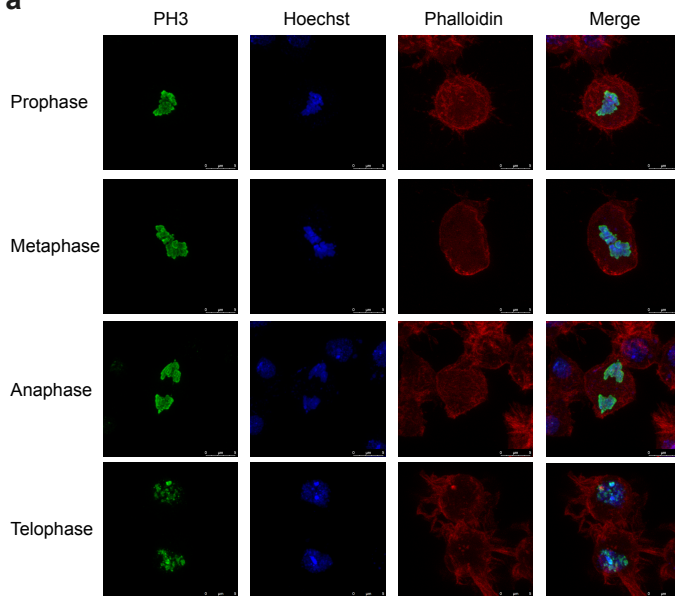
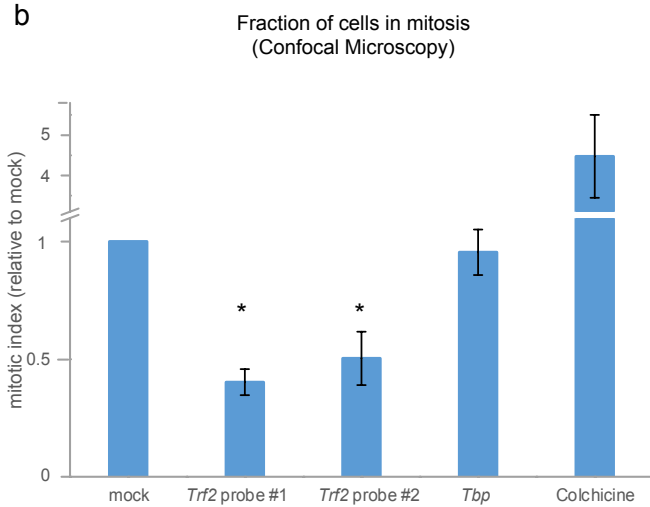
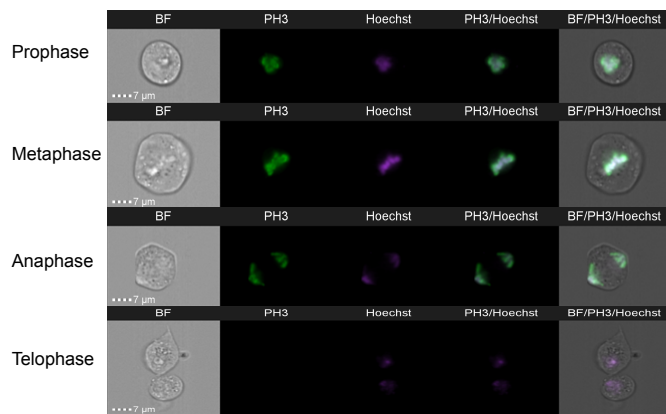
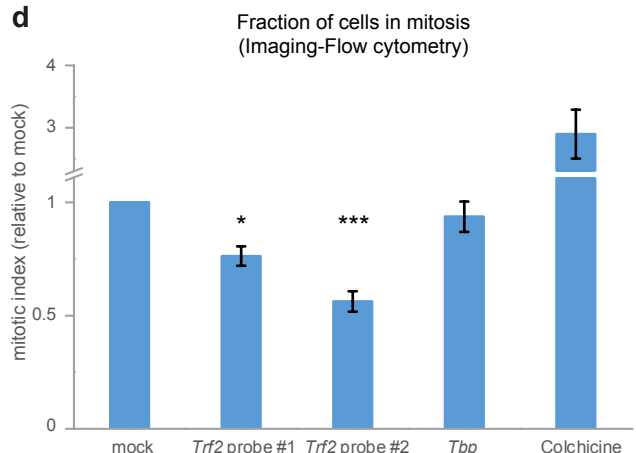
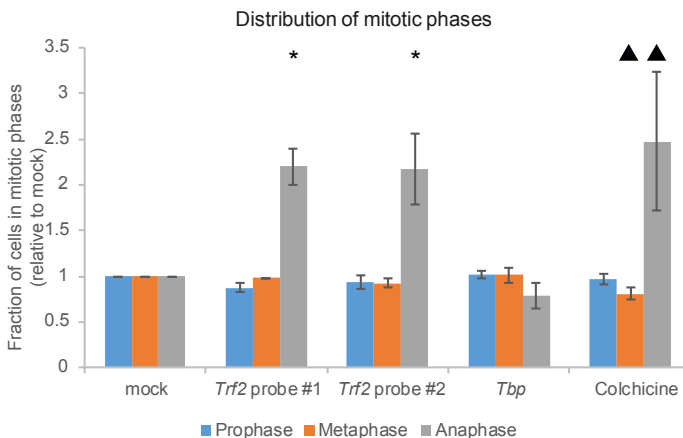
**a****b**



**a****b**



**a****b****c**

**a****b****c****d****e****f**